Natural Resources Canada
Ressources naturelles Canada

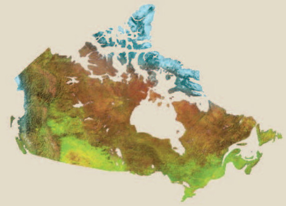

U-Pb ages of Archean basement and Paleoproterozoic plutonic rocks, southern Cumberland Peninsula, eastern Baffin Island, Nunavut

N.M. Rayner, M. Sanborn-Barrie, M.D. Young, and J.B. Whalen

Geological Survey of Canada
Current Research 2012-8

2012

Canada

Geological Survey of Canada
Current Research 2012-8

U-Pb ages of Archean basement and Paleoproterozoic plutonic rocks, southern Cumberland Peninsula, eastern Baffin Island, Nunavut

N.M. Rayner, M. Sanborn-Barrie, M.D. Young, and J.B. Whalen

2012

ISSN 1701-4387
Catalogue No. M44-2012/8E-PDF
ISBN 978-1-100-20684-4
doi:10.4095/291401

A copy of this publication is also available for reference in depository libraries across Canada through access to the Depository Services Program's Web site at http://dsp-psd.pwgsc.gc.ca

This publication is available for free download through GEOSCAN
http://geoscan.ess.nrcan.gc.ca

Toll-free (Canada and U.S.A.): 1-888-252-4301

Recommended citation

Rayner, N.M., Sanborn-Barrie, M., Young, M.D., and Whalen, J.B., 2012. U-Pb ages of Archean basement and Paleoproterozoic plutonic rocks, southern Cumberland Peninsula, eastern Baffin Island, Nunavut; Geological Survey of Canada, Current Research 2012-8, 24 p. doi: 10.4095/291401

Critical review

N. Wodicka

Authors

N.M. Rayner (Nicole.Rayner@NRCan-RNCan.gc.ca)
M. Sanborn-Barrie (Mary.Sanborn-Barrie@NRCan-RNCan.gc.ca)
J.B. Whalen (Joe.Whalen@NRCan-RNCan.gc.ca)
Geological Survey of Canada
601 Booth Street
Ottawa, Ontario
K1A 0E8

M.D. Young (MDYoung@Dal.ca)
Department of Earth Sciences
Dalhousie University
1459 Oxford Street
P.O. Box 15 000
Halifax, Nova Scotia
B3H 4R2

Correction date:

U-Pb ages of Archean basement and Paleoproterozoic plutonic rocks, southern Cumberland Peninsula, eastern Baffin Island, Nunavut

N.M. Rayner, M. Sanborn-Barrie, M.D. Young, and J.B. Whalen

Rayner, N.M., Sanborn-Barrie, M., Young, M.D., and Whalen, J.B., 2012. U-Pb ages of Archean basement and Paleoproterozoic plutonic rocks, southern Cumberland Peninsula, eastern Baffin Island, Nunavut; Geological Survey of Canada, Current Research 2012-8, 24 p. doi: 10.4095/291401

Abstract: Recent mapping coupled with geochronological and isotopic studies on the southern half of Cumberland Peninsula, Baffin Island, have identified and characterized four distinct plutonic suites. An extensive plutonic gneiss complex yields ages of 2991 ± 4 Ma, 2938 ± 4 Ma, and 2782 ± 4 Ma, whereas a second group of discrete plutons yields solely Neoarchean ages of 2772 ± 6 Ma, 2759 ± 3 Ma, and 2700 ± 4 Ma. These Archean rocks form the structural basement to a cover sequence, the Hoare Bay Group, both of which are cut by a charnockite-granodiorite-diorite suite with ages of 1894 ± 5 Ma and 1889 ± 3 Ma, informally designated the Qikiqtarjuaq plutonic suite. Mylonitic, high-K intrusive sheets, interpreted to have been emplaced syntectonically during regional deformation, yield ages of 1882 ± 13 Ma and 1873 ± 16 Ma.

Résumé : De récents travaux cartographiques dans la moitié sud de la péninsule Cumberland, sur l'île de Baffin, combinés à des études géochronologiques et isotopiques, ont permis d'identifier et de caractériser quatre suites plutoniques distinctes. Des datations effectuées sur un vaste complexe gneissique d'origine plutonique ont fourni des âges de 2991 ± 4 Ma, 2938 ± 4 Ma et 2782 ± 4 Ma, alors qu'un second groupe de plutons distincts a livré uniquement des âges néoarchéens, soit 2772 ± 6 Ma, 2759 ± 3 Ma et 2700 ± 4 Ma. Ces roches archéennes forment le socle structural d'une séquence de couverture, le Groupe de Hoare Bay; ces deux entités sont recoupées par une suite de charnockite-granodiorite-diorite, appelée de façon informelle suite plutonique de Qikiqtarjuaq, qui a livré des âges de 1894 ± 5 et 1889 ± 3 Ma. Des feuillets mylonitiques intrusifs à haute teneur en potassium, dont la mise en place syntectonique aurait eu lieu pendant la déformation régionale, ont donné des âges de 1882 ± 13 Ma et 1873 ± 16 Ma.

INTRODUCTION

Framework geoscience mapping of Cumberland Peninsula, eastern Baffin Island, was undertaken during the summers of 2009 and 2010 as part of NRCan's Geomapping for Energy and Minerals (GEM) initiative. Prior to this, significant geoscience knowledge gaps existed due to limited and outdated mapping, as well as scant isotopic information. New maps (Sanborn-Barrie et al., 2011a, b, c), in conjunction with the geochronological results presented here, have resulted in a vastly improved understanding of the lithological associations, crustal architecture, and mineral potential of this part of the eastern Canadian Arctic.

It is now recognized that variably foliated to gneissic plutonic rocks underlie about 60% of Cumberland Peninsula and dominate its southern part (Fig. 1). Narrow strands of Archean supracrustal rocks including semipelite, amphibolite, rare pillowed volcanic rocks, and porphyry form a minor, yet significant lithological component in the south. Supracrustal rocks of a Paleoproterozoic cover sequence, the Hoare Bay Group, form a coherent succession of clastic and chemical metasedimentary rocks across the central part of the peninsula (Fig. 1). Where the basement-cover contact is exposed, strongly deformed metasedimentary rocks, devoid of primary depositional features, are in contact with concordant plutonic mylonite gneiss. Both the basement complex and cover sequence are cut by foliated, locally K-feldspar porphyritic granodiorite±charnockite±quartz dioritic plutons. Fabrics and structures in the basement complex provide evidence of two regionally developed penetrative deformation events, the youngest of which is also recorded in the cover sequence.

This report focuses on the geochronology and geological significance of plutonic rocks of southern Cumberland Peninsula.

ANALYTICAL METHODS

Sample preparation and SHRIMP analytical procedures followed those described by Stern (1997), with standards and U-Pb calibration methods following Stern and Amelin (2003). The internal features of the zircon grains (such as zoning, structures, alteration, etc.) were characterized in back-scattered electron mode utilizing a Zeiss Evo 50 scanning electron microscope. Footnotes supplied on the accompanying data table (Table 1) highlight analytical details for each session. Off-line data processing was accomplished using SQUID2. Common Pb correction utilized the Pb composition of the surface blank (Stern, 1997). Data from some sessions required a mass fractionation correction to the Pb-isotope data, the magnitude of which was determined from the measurement of secondary standard z1242 (accepted $^{207}Pb/^{206}Pb$ age = 2681 Ma, B. Davis, pers. comm. (2010)). *See* footnote to Table 1 for details on the mass fractionation correction. Isoplot v. 3.00 (Ludwig, 2003) was used to generate concordia plots and to calculate weighted means. The error ellipses on the concordia diagrams and the weighted mean errors are reported at 2σ.

TARGETED SAMPLES

The predominant lithology exposed throughout the southern part of the map area is strongly foliated to gneissic tonalite to granodiorite in which gneissic banding is typically attributed to high strain and concordant felsic injections (Fig. 2a). Three samples (09SRB-B76A, 09SRB-M106A, 09SRB-M100A) were collected to constrain the age of the gneiss complex, and one of these (09SRB-M100A) displayed an intrusive relationship to metasedimentary rocks, thereby also providing a minimum age for supracrustal panels exposed across the southern part of the peninsula. This region also exposes homogeneous, variably foliated, aeromagnetically delineated plutons, sampled at three localities (10SRB-M197, 09SRB-D042A, 09SRB-D040B). Plutonic rocks that cut the Hoare Bay Group (Jackson, 1971; St-Onge et al., 2006) form a 200 km long plutonic belt, exposed between Pangnirtung and Qikiqtarjuaq (Fig. 1). Two samples (07SAB-002, 09SRB-M109A) were targeted to constrain the timing of this plutonic belt and test whether it represents part of the 1.865–1.845 Ga Cumberland Batholith (Whalen et al., 2010). Lastly, mylonitic sheets proximal to the contact between the plutonic gneiss complex and the Hoare Bay Group were dated at two localities (09SRB-D010C, 09SRB-M145) to determine the timing of magmatism and deformation near the apparent basement-cover contact.

RESULTS

09SRB-B076A (GSC lab number z9971)

In order to constrain the age of the oldest component of the gneiss complex, a relatively homogenous tonalitic layer from a grey tonalite to granodiorite banded gneiss was collected (Fig. 2a). It yielded elongate prismatic, colourless to pale yellow zircon with few inclusions, but significant fracturing. Back-scattered electron imaging of the zircon grains reveals faint, 10–20 μm zoning in their inner regions and occasionally finer scale (sub-micrometre), parallel zoning toward the grain edge. Twenty-four SHRIMP analyses were carried out on 22 individual zircon grains yielding ages ranging from 3005–2884 Ma (Fig. 2b). The sixteen oldest analyses form a single population with a weighted mean $^{207}Pb/^{206}Pb$ age of 2991 ± 4 Ma, interpreted as the time of crystallization. The remaining eight analyses scatter sporadically to younger ages, with no age predominating. One of these younger analyses is a duplicate analysis of a grain that

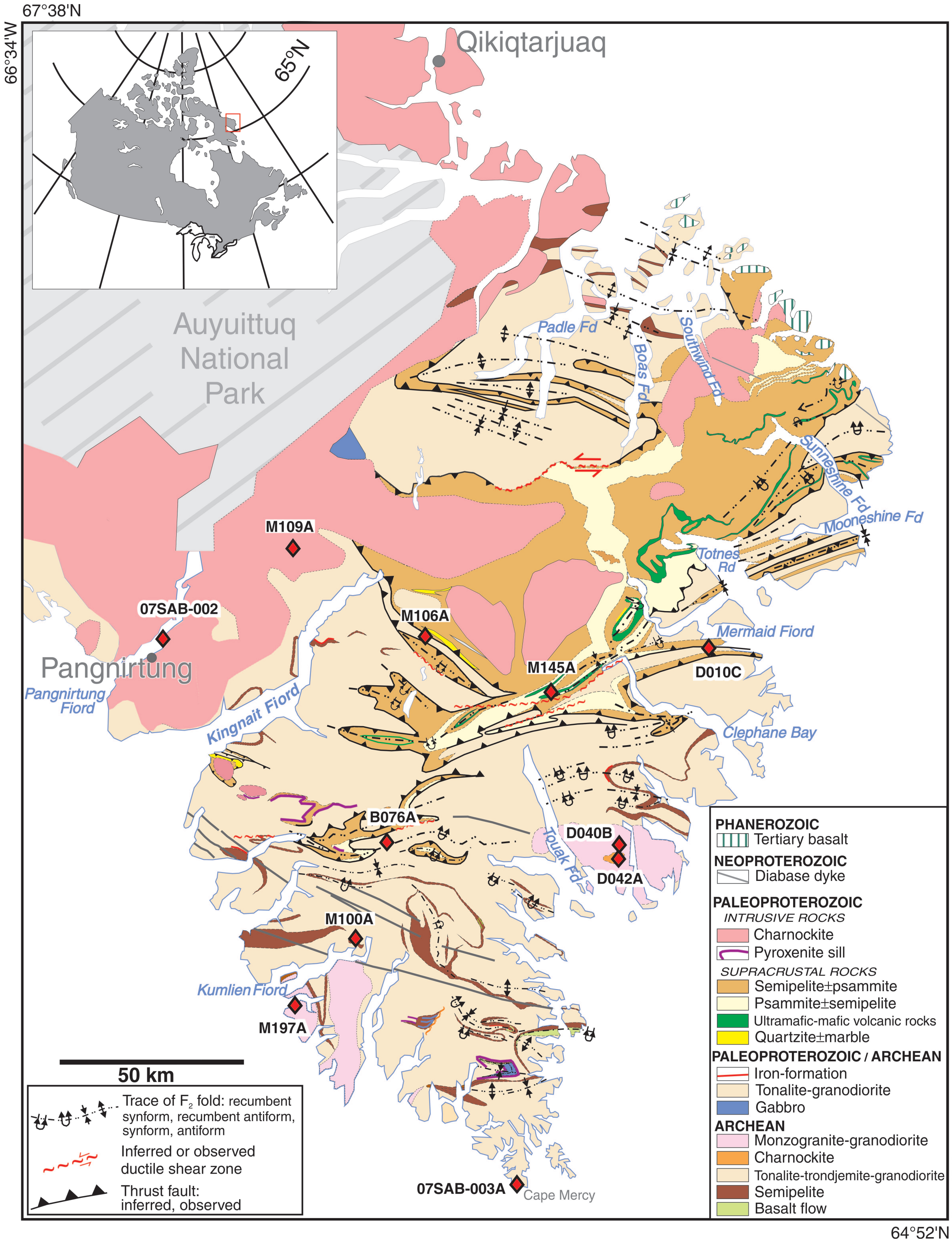

Figure 1. Simplified geological map of Cumberland Peninsula (*after* Sanborn-Barrie et al., 2011a, b, c). Abbreviated sample names shown; complete names are found in text and table.

Table 1. SHRIMP U-Pb results.

Spot name	U (ppm)	Th (ppm)	Th/U	Yb (ppm)	Hf (ppm)	^{204}Pb/^{206}Pb	% ±	f(206)^{204} %	^{206}Pb* (ppm)	^{208*}Pb/^{206*}Pb	% ±	^{207*}Pb/^{235}U	% ±	^{206*}Pb/^{238}U	% ±	Corr Coeff	^{207*}Pb/^{206*}Pb	% ±	Apparent ages (Ma): ^{206}Pb/^{238}U	±^{206}Pb/^{238}U	^{207}Pb/^{206}Pb	±^{207}Pb/^{206}Pb	Disc. (%)
09SRB-B076A(GSC lab number z9971) IP559; NAD83: 65.71959N, -64.39622W																							
9971-29.1	653	121	0.19	nd	nd	0.000190	22	0.33	306	0.057	3.7	15.561	1.4	0.5448	1.3	0.9585	0.2072	0.39	2803	30	2884	6	3.4
9971-21.1	595	53	0.09	nd	nd	0.000041	44	0.07	289	0.021	6.6	16.242	1.4	0.5642	1.3	0.9686	0.2088	0.34	2884	31	2896	5	0.5
9971-27.1	377	188	0.52	nd	nd	0.000077	30	0.13	187	0.145	3.2	16.953	1.5	0.5771	1.4	0.9623	0.2131	0.41	2937	34	2929	7	-0.3
9971-22.1	572	289	0.52	nd	nd	0.000042	40	0.07	276	0.142	2.6	16.656	1.4	0.5613	1.3	0.9706	0.2152	0.33	2872	30	2945	5	3.1
9971-33.2	394	260	0.68	nd	nd	0.000030	40	0.05	177	0.191	3.4	15.628	1.5	0.5229	1.4	0.9463	0.2168	0.47	2711	31	2957	8	10.2
9971-33.1	468	357	0.79	nd	nd	0.000029	137	0.05	231	0.218	2.4	17.189	1.4	0.5745	1.3	0.9314	0.2170	0.52	2926	31	2959	8	1.4
9971-1.1	396	235	0.61	nd	nd	0.000021	36	0.04	189	0.177	2.8	16.643	1.4	0.5552	1.3	0.9626	0.2174	0.38	2847	31	2962	6	4.8
9971-34.1	396	242	0.63	nd	nd	0.000082	33	0.14	179	0.174	3.2	15.811	1.4	0.5256	1.4	0.9500	0.2182	0.44	2723	30	2967	7	10.1
9971-22.2	431	309	0.74	nd	nd	0.000042	40	0.07	208	0.195	2.9	17.036	1.4	0.5616	1.4	0.9569	0.2200	0.41	2873	31	2981	7	4.5
9971-4.1	318	164	0.53	nd	nd	0.000000	100	0.00	155	0.144	3.5	17.232	1.4	0.5680	1.4	0.9570	0.2200	0.42	2900	32	2981	7	3.4
9971-36.1	443	285	0.66	nd	nd	0.000050	41	0.09	216	0.200	2.9	17.207	1.4	0.5665	1.3	0.9557	0.2203	0.41	2893	31	2983	7	3.7
9971-38.1	1190	809	0.70	nd	nd	0.000077	25	0.13	604	0.185	1.6	17.986	1.4	0.5910	1.3	0.9308	0.2207	0.51	2994	31	2986	8	-0.3
9971-35.1	355	175	0.51	nd	nd	0.000044	22	0.08	183	0.143	3.3	18.212	1.4	0.5984	1.4	0.9594	0.2207	0.40	3023	33	2986	6	-1.6
9971-26.1	408	267	0.68	nd	nd	0.000019	40	0.03	205	0.179	2.8	17.889	1.4	0.5870	1.3	0.9646	0.2210	0.37	2977	32	2988	6	0.5
9971-2.1	578	326	0.58	nd	nd	0.000011	47	0.02	289	0.166	2.5	17.760	1.4	0.5823	1.3	0.9710	0.2212	0.32	2958	31	2990	5	1.3
9971-14.1	417	307	0.76	nd	nd	0.000014	144	0.02	214	0.185	2.6	18.215	1.6	0.5970	1.5	0.9732	0.2213	0.36	3018	36	2990	6	-1.2
9971-18.1	449	310	0.71	nd	nd	0.000000	100	0.00	220	0.191	2.7	17.451	1.4	0.5718	1.3	0.9657	0.2213	0.36	2915	31	2990	6	3.1
9971-25.1	429	237	0.57	nd	nd	0.000260	22	0.45	210	0.157	2.9	17.369	1.4	0.5690	1.3	0.9400	0.2214	0.49	2904	31	2991	8	3.6
9971-8.1	469	368	0.81	nd	nd	0.000015	40	0.03	238	0.212	2.3	18.016	1.4	0.5901	1.3	0.9692	0.2214	0.34	2990	32	2991	5	0.1
9971-13.1	465	285	0.63	nd	nd	0.000072	33	0.12	225	0.176	4.1	17.224	1.4	0.5634	1.4	0.9658	0.2217	0.37	2881	32	2993	6	4.7
9971-12.1	538	519	1.00	nd	nd	0.000000	100	0.00	279	0.282	1.9	18.501	1.4	0.6039	1.3	0.9735	0.2222	0.31	3046	32	2997	5	-2.1
9971-7.1	561	356	0.65	nd	nd	0.000009	47	0.02	272	0.179	2.4	17.325	1.4	0.5653	1.4	0.9747	0.2223	0.32	2889	32	2997	5	4.5
9971-19.1	381	274	0.74	nd	nd	0.000017	140	0.03	205	0.197	2.8	19.218	1.5	0.6248	1.4	0.9635	0.2231	0.40	3129	36	3003	6	-5.3
9971-16.1	505	319	0.65	nd	nd	0.000000	100	0.00	261	0.182	2.5	18.561	1.4	0.6027	1.3	0.9596	0.2234	0.39	3041	32	3005	6	-1.5
09SRB-M106A (GSC lab number z10464) IP609; NAD83: 66.20447N, -64.10985W																							
10464-35.2	810	56	0.07	274	12724	0.000217	12	0.38	338	0.012	3.6	10.566	1.2	0.4863	1.2	0.9632	0.1576	0.33	2555	25	2430	6	-6.2
10464-53.2	619	78	0.13	336	14576	0.000165	18	0.29	283	0.030	3.7	12.935	1.3	0.5317	1.2	0.9620	0.1764	0.34	2749	27	2620	6	-6.1
10464-55.1	1030	20	0.02	288	16445	0.000091	13	0.16	444	0.005	3.5	12.353	1.2	0.5016	1.2	0.9890	0.1786	0.18	2621	25	2640	3	0.9
10464-22.1	1318	37	0.03	611	15371	0.000001	852	0.00	591	0.008	2.9	13.090	1.2	0.5222	1.2	0.9861	0.1818	0.20	2708	26	2669	3	-1.8
10464-64.2	913	37	0.04	564	15059	0.000025	21	0.04	433	0.011	2.6	14.108	1.2	0.5524	1.2	0.9890	0.1852	0.18	2835	27	2700	3	-6.2
10464-94.3	414	69	0.17	391	13385	0.000466	6	0.81	196	0.049	1.7	14.096	1.2	0.5510	1.2	0.9712	0.1855	0.29	2829	27	2703	5	-5.8
10464-86.1	1003	39	0.04	319	18538	0.000083	11	0.14	484	0.004	6.3	14.545	1.2	0.5615	1.2	0.9885	0.1879	0.18	2873	27	2724	3	-6.8
10464-94.1	334	61	0.19	391	15532	0.000003	89	0.01	149	0.054	2.5	13.540	1.3	0.5182	1.2	0.9436	0.1895	0.42	2692	26	2738	7	2.1
10464-46.2	206	120	0.60	288	7945	0.000023	141	0.04	101	0.169	1.7	16.427	1.3	0.5723	1.2	0.9575	0.2082	0.36	2917	28	2891	6	-1.1
10464-46.1	182	78	0.44	190	8013	-0.000039	69	-0.07	88	0.125	2.2	16.295	1.4	0.5634	1.2	0.8799	0.2098	0.66	2881	29	2904	11	1.0
10464-2.1	352	204	0.60	252	8875	0.000009	25	0.02	171	0.170	1.3	16.424	1.3	0.5663	1.3	0.9830	0.2103	0.23	2893	29	2908	4	0.7
10464-40.1	431	182	0.44	360	11199	0.000007	67	0.01	207	0.124	1.3	16.184	1.2	0.5579	1.2	0.9848	0.2104	0.21	2858	27	2908	3	2.1
10464-36.1	465	281	0.62	298	10167	0.000006	186	0.01	225	0.173	1.1	16.304	1.4	0.5621	1.2	0.8938	0.2104	0.62	2875	28	2909	10	1.4
10464-19.1	446	223	0.52	291	10339	0.000031	29	0.05	212	0.145	1.2	16.057	1.2	0.5533	1.2	0.9847	0.2105	0.21	2839	27	2909	3	3.0
10464-17.1	318	192	0.62	243	8775	0.000012	84	0.02	156	0.172	1.3	16.639	1.3	0.5707	1.2	0.9806	0.2115	0.25	2911	29	2917	4	0.3
10464-5.1	207	77	0.38	220	8417	0.000045	33	0.08	103	0.109	2.1	16.883	1.2	0.5778	1.2	0.9653	0.2119	0.33	2940	28	2920	5	-0.8
10464-10.1	171	90	0.54	180	8093	0.000013	85	0.02	85	0.151	1.9	16.963	1.3	0.5801	1.3	0.9676	0.2121	0.33	2949	30	2921	5	-1.2
10464-25.1	307	141	0.47	301	9121	0.000006	286	0.01	152	0.133	1.6	16.862	1.2	0.5764	1.2	0.9743	0.2122	0.28	2934	28	2922	4	-0.5
10464-89.1	221	124	0.58	195	8633	0.000055	83	0.09	108	0.154	1.7	16.675	1.3	0.5696	1.2	0.9523	0.2123	0.39	2906	28	2923	6	0.7
10464-18.1	165	54	0.34	198	8250	-0.000022	67	-0.04	80	0.090	2.6	16.499	1.3	0.5628	1.2	0.9605	0.2126	0.35	2878	28	2926	6	2.0
10464-4.1	304	185	0.63	242	8530	0.000013	42	0.02	152	0.178	1.3	17.103	1.2	0.5828	1.2	0.9800	0.2128	0.24	2960	28	2927	4	-1.4
10464-94.2	278	183	0.68	220	7982	0.000005	349	0.01	143	0.189	1.3	17.551	1.3	0.5980	1.3	0.9783	0.2128	0.27	3022	30	2927	4	-4.0
10464-64.1	282	150	0.55	378	8580	0.000010	89	0.02	134	0.152	1.7	16.217	1.2	0.5525	1.2	0.9704	0.2129	0.30	2835	27	2928	5	3.9
10464-14.1	246	135	0.57	206	8345	-0.000005	200	-0.01	120	0.160	1.6	16.778	1.2	0.5707	1.2	0.9710	0.2132	0.29	2911	28	2930	5	0.8
10464-35.1	237	135	0.59	314	8145	0.000030	22	0.05	115	0.159	1.6	16.601	1.2	0.5640	1.2	0.9716	0.2135	0.29	2883	28	2932	5	2.1
10464-1.1	349	155	0.46	279	9498	0.000019	20	0.03	176	0.128	1.4	17.298	1.3	0.5875	1.2	0.9473	0.2135	0.42	2979	29	2933	7	-2.0
10464-30.1	235	132	0.58	210	8012	0.000014	22	0.03	111	0.157	1.7	16.195	1.2	0.5496	1.2	0.9701	0.2137	0.30	2823	27	2934	5	4.7
10464-36.2	301	115	0.40	294	9071	0.000014	24	0.02	143	0.110	1.9	16.325	1.2	0.5533	1.2	0.9734	0.2140	0.28	2839	27	2936	5	4.1

Table 1. Continued.

Spot name	U (ppm)	Th (ppm)	Th/U	Yb (ppm)	Hf (ppm)	^{204}Pb/^{206}Pb	% ±	f(206)^{204} %	^{206}Pb* (ppm)	^{208*}Pb/^{206*}Pb	% ±	^{207*}Pb/^{235}U	% ±	^{206*}Pb/^{238}U	% ±	Corr Coeff	^{207*}Pb/^{206*}Pb	% ±	Apparent ages (Ma) ^{206}Pb/^{238}U	±^{206}Pb/^{238}U	^{207}Pb/^{206}Pb	±^{207}Pb/^{206}Pb	Disc. (%)
09SRB-M106A (GSC lab number z10464) IP609; NAD83: 66.20447N, -64.10985W (continued)																							
10464-3.1	175	66	0.39	187	8206	0.000000	100	0.00	89	0.107	2.2	17.429	1.2	0.5906	1.2	0.9652	0.2140	0.33	2992	29	2936	5	-2.4
10464-53.1	247	126	0.53	284	8651	0.000073	31	0.13	120	0.133	1.7	16.702	1.2	0.5658	1.2	0.9696	0.2141	0.30	2890	28	2937	5	2.0
10464-24.1	249	148	0.61	381	8088	0.000012	129	0.02	121	0.172	1.5	16.696	1.4	0.5655	1.4	0.9788	0.2141	0.30	2889	33	2937	5	2.0
10464-47.2	368	220	0.62	257	9355	0.000007	45	0.01	177	0.173	1.3	16.557	1.2	0.5607	1.2	0.9794	0.2142	0.25	2869	28	2937	4	2.9
10464-39.2	274	160	0.60	213	8203	0.000003	852	0.00	135	0.166	1.5	17.035	1.2	0.5759	1.2	0.9705	0.2146	0.30	2932	28	2940	5	0.4
10464-47.1	322	140	0.45	274	9587	0.000010	97	0.02	157	0.122	1.5	16.782	1.3	0.5671	1.2	0.9811	0.2146	0.24	2896	29	2941	4	1.9
10464-90.1	175	58	0.34	208	9049	0.000057	80	0.10	88	0.089	2.4	17.314	1.3	0.5850	1.2	0.9487	0.2147	0.41	2969	29	2941	7	-1.2
10464-39.1	175	86	0.51	238	8171	0.000004	73	0.01	88	0.143	1.9	17.438	1.2	0.5874	1.2	0.9655	0.2153	0.33	2979	29	2946	5	-1.4
10464-12.1	184	84	0.47	209	7923	0.000027	29	0.05	92	0.128	1.9	17.312	1.2	0.5803	1.2	0.9700	0.2164	0.30	2950	29	2954	5	0.2
09SRB-M100A (GSC lab number z9979) IP539; NAD83: 65.46097N, -64.48530W																							
9979-85.2	1598	33	0.02	nd	nd	0.000058	12	0.10	640	0.006	3.5	10.295	1.2	0.4663	1.2	0.9914	0.1601	0.15	2467	24	2457	3	-0.5
9979-83.1	1389	28	0.02	nd	nd	0.000013	97	0.02	560	0.007	4.7	10.634	1.2	0.4698	1.2	0.9855	0.1642	0.20	2483	24	2499	3	0.8
9979-49.2	1904	276	0.15	nd	nd	0.000168	6	0.29	869	0.049	1.2	13.715	1.2	0.5316	1.2	0.9928	0.1871	0.14	2748	26	2717	2	-1.4
9979-45.1	1546	433	0.29	nd	nd	0.000004	113	0.01	726	0.083	1.1	14.262	1.2	0.5467	1.2	0.9699	0.1892	0.29	2811	27	2735	5	-3.4
9979-3.1	274	30	0.11	nd	nd	0.000057	62	0.10	119	0.034	3.6	13.336	1.3	0.5083	1.2	0.9606	0.1903	0.36	2650	27	2745	6	4.2
9979-38.1	907	141	0.16	nd	nd	0.000111	11	0.19	373	0.049	1.8	12.685	1.2	0.4790	1.2	0.9875	0.1921	0.19	2523	25	2760	3	10.4
9979-85.1	106	251	2.46	nd	nd	0.000262	25	0.45	47	0.720	1.5	13.669	1.6	0.5159	1.4	0.9098	0.1921	0.66	2682	32	2761	11	3.5
9979-16.1	327	71	0.22	nd	nd	0.000023	93	0.04	151	0.064	2.5	14.369	1.3	0.5395	1.2	0.9334	0.1932	0.47	2781	28	2769	8	-0.5
9979-52.1	339	274	0.84	nd	nd	0.000036	37	0.06	163	0.229	1.2	14.901	1.3	0.5589	1.2	0.9674	0.1934	0.32	2862	28	2771	5	-4.1
9979-60.1	376	169	0.46	nd	nd	0.000016	75	0.03	176	0.129	1.5	14.578	1.2	0.5450	1.2	0.9820	0.1940	0.23	2804	27	2776	4	-1.2
9979-73.1	1564	659	0.44	nd	nd	0.000008	43	0.01	749	0.122	0.7	14.917	1.2	0.5572	1.2	0.9865	0.1942	0.19	2855	27	2778	3	-3.4
9979-58.1	372	86	0.24	nd	nd	0.000071	16	0.12	174	0.065	2.0	14.585	1.2	0.5442	1.2	0.9823	0.1944	0.23	2801	27	2779	4	-1.0
9979-70.1	181	82	0.47	nd	nd	0.000032	32	0.06	83	0.133	2.2	14.343	1.3	0.5348	1.3	0.9683	0.1945	0.33	2761	29	2781	5	0.9
9979-24.1	618	120	0.20	nd	nd	0.000003	359	0.00	282	0.053	2.0	14.263	1.2	0.5317	1.2	0.9755	0.1945	0.27	2749	27	2781	4	1.4
9979-55.1	240	66	0.28	nd	nd	0.000073	27	0.13	115	0.080	2.3	14.908	1.3	0.5557	1.3	0.9752	0.1946	0.30	2849	30	2781	5	-3.0
9979-43.2	214	89	0.43	nd	nd	0.000022	93	0.04	96	0.128	2.1	13.956	2.1	0.5200	2.0	0.9771	0.1946	0.44	2699	44	2782	7	3.6
9979-7.1	674	223	0.34	nd	nd	0.000014	59	0.03	311	0.095	1.4	14.410	1.2	0.5367	1.2	0.9733	0.1947	0.28	2770	27	2782	5	0.6
9979-1.1	551	151	0.28	nd	nd	0.000004	399	0.01	260	0.080	1.6	14.812	1.5	0.5496	1.4	0.9863	0.1955	0.24	2823	33	2789	4	-1.5
9979-64.1	465	176	0.39	nd	nd	0.000022	50	0.04	218	0.110	1.7	14.735	1.3	0.5466	1.2	0.9772	0.1955	0.27	2811	28	2789	4	-1.0
9979-6.1	511	109	0.22	nd	nd	-0.000023	61	-0.04	237	0.062	2.0	14.561	1.2	0.5385	1.2	0.9832	0.1961	0.22	2777	27	2794	4	0.7
9979-66.1	177	47	0.28	nd	nd	0.000045	140	0.08	82	0.081	2.6	14.566	1.4	0.5375	1.3	0.9230	0.1965	0.53	2773	29	2798	9	1.1
9979-39.1	617	163	0.27	nd	nd	0.000011	37	0.02	286	0.077	1.6	14.671	1.3	0.5393	1.3	0.9820	0.1973	0.25	2781	29	2804	4	1.0
9979-49.1	493	218	0.46	nd	nd	0.000051	26	0.09	236	0.142	1.3	15.752	1.2	0.5579	1.2	0.9786	0.2048	0.25	2858	28	2865	4	0.3
9979-8.2	1473	291	0.20	nd	nd	0.000162	6	0.28	767	0.063	1.1	17.130	1.2	0.6060	1.2	0.9940	0.2050	0.13	3054	28	2866	2	-8.2
9979-48.1	111	28	0.26	nd	nd	0.000064	54	0.11	55	0.081	3.2	16.374	1.6	0.5768	1.5	0.9370	0.2059	0.55	2936	35	2873	9	-2.7
9979-31.1	261	75	0.30	nd	nd	0.000019	60	0.03	126	0.086	2.4	16.055	1.3	0.5607	1.3	0.9743	0.2077	0.29	2870	29	2887	5	0.8
10SRB-M197A (GSC lab number z10462) IP604; NAD83: 65.32232 N, -64.84211W																							
10462-56.2	801	27	0.03	70	10665	0.000113	13	0.20	357	0.006	4.1	12.791	1.4	0.5194	1.4	0.9866	0.1786	0.24	2697	32	2640	4	-2.6
10462-41.1	273	80	0.30	97	9725	0.000010	80	0.02	112	0.083	2.3	11.980	1.5	0.4797	1.5	0.9758	0.1811	0.33	2526	30	2663	5	6.2
10462-11.2	943	196	0.21	110	10226	0.000338	14	0.59	442	0.031	5.1	13.651	1.6	0.5458	1.5	0.9640	0.1814	0.43	2808	35	2666	7	-6.6
10462-35.2	221	56	0.26	82	9825	0.000044	34	0.08	94	0.073	2.9	12.503	1.5	0.4972	1.5	0.9655	0.1824	0.40	2602	31	2675	7	3.3

Notes (*see* Stern, 1997):
Spot name follows the convention x-y.z; where x = sample number, y = grain number, and z = spot number. Multiple analyses in an individual spot are labelled as x-y.z.z
Uncertainties reported at 1s and are calculated by using SQUID 2.23.08.10.21, rev. 21 Oct 2008
nd = not determined
f206^{204} refers to mole percent of total ^{206}Pb that is due to common Pb, calculated using the ^{204}Pb-method; common Pb composition used is the surface blank (4/6: 0.05770; 7/6: 0.89500; 8/6: 2.13840)
* refers to radiogenic Pb (corrected for common Pb)
Discordance relative to origin = 100 * ((207/206 age -206/238 age)/(^{207}Pb/^{206}Pb age))
Calibration standard 6266; U = 910 ppm; Age = 559 Ma; ^{206}Pb/^{238}U = 0.09059

Analytical details
IP539: 26 µm spot; 5 scans; U-Pb calibration error 1.15% (included);
Measured age of secondary standard 1242 = 2685 ± 4 Ma (n = 15); no mass fractionation correction.
IP559: 16 µm spot; 5 scans; U-Pb calibration error 1.23% (included);
Measured age of secondary standard 1242 = 2677 ± 8 Ma (n = 16); no mass fractionation correction.
IP604: 23 µm spot; 6 scans; U-Pb calibration error 1.41% (included);
Measured age of secondary standard 1242 = 2679 ± 4 Ma (n = 21); no mass fractionation correction.
IP609: 23 µm spot; 6 scans; U-Pb calibration error 1.17% (included);
Measured age of secondary standard 1242 = 2675 ± 3 Ma (n = 37); Intraelement mass fractionation correction of 0.3% applied to unknowns.

Table 1. Continued.

Spot name	U (ppm)	Th (ppm)	Th/U	Yb (ppm)	Hf (ppm)	$^{204}Pb/^{206}Pb$	% ±	$f(206)^{204}$ %	$^{206}Pb^*$ (ppm)	$^{208*}Pb/^{206*}Pb$	% ±	$^{207*}Pb/^{235}U$	% ±	$^{206*}Pb/^{238}U$	% ±	Corr Coeff	$^{207*}Pb/^{206*}Pb$	% ±	Apparent ages (Ma) $^{206}Pb/^{238}U$	$\pm^{206}Pb/^{238}U$	$^{207}Pb/^{206}Pb$	$\pm^{207}Pb/^{206}Pb$	Disc. (%)
10SRB-M197A (GSC lab number z10462) IP604; NAD83: 65.32232 N, -64.84211W (continued)																							
10462-22.1	1228	454	0.38	102	12532	0.000254	6	0.44	532	0.007	2.5	12.935	1.4	0.5040	1.4	0.9909	0.1861	0.19	2631	31	2708	3	3.5
10462-7.1	222	92	0.43	59	8633	0.000106	24	0.18	97	0.114	2.1	13.087	1.5	0.5096	1.5	0.9673	0.1863	0.38	2655	32	2709	6	2.4
10462-31.1	226	85	0.39	89	9032	0.000049	60	0.08	98	0.097	2.3	13.086	1.7	0.5058	1.6	0.9455	0.1876	0.55	2639	35	2722	9	3.7
10462-33.1	1166	109	0.10	173	10686	0.000010	19	0.02	535	0.026	1.9	13.857	1.5	0.5343	1.4	0.9624	0.1881	0.41	2760	32	2725	7	-1.5
10462-54.1	174	47	0.28	64	11025	0.000051	17	0.09	76	0.078	3.0	13.183	1.7	0.5075	1.7	0.9708	0.1884	0.42	2646	37	2728	7	3.7
10462-10.1	419	110	0.27	127	10159	0.000025	28	0.04	185	0.076	1.9	13.369	1.5	0.5126	1.4	0.9850	0.1892	0.25	2668	32	2735	4	3.0
10462-90.1	1063	95	0.09	120	11211	0.000019	35	0.03	493	0.023	2.1	14.088	1.4	0.5396	1.4	0.9929	0.1894	0.17	2782	32	2737	3	-2.0
10462-43.1	317	55	0.18	96	10234	-0.000016	72	-0.03	145	0.050	2.8	13.940	1.9	0.5336	1.9	0.9865	0.1895	0.31	2756	42	2738	5	-0.8
10462-31.2	229	75	0.34	88	8868	0.000054	21	0.09	107	0.093	4.2	14.245	1.5	0.5448	1.5	0.9711	0.1897	0.37	2803	34	2739	6	-2.9
10462-53.1	317	239	0.78	77	9530	0.000023	73	0.04	146	0.216	1.4	14.013	1.5	0.5347	1.5	0.9757	0.1901	0.33	2761	33	2743	5	-0.8
10462-33.2	1195	89	0.08	124	11013	-0.000004	0	-0.01	526	0.021	2.2	13.519	1.5	0.5128	1.5	0.9938	0.1912	0.16	2669	32	2752	3	3.7
10462-50.1	340	100	0.30	111	9728	0.000207	13	0.36	163	0.080	2.0	14.749	1.5	0.5592	1.5	0.9749	0.1913	0.34	2864	35	2753	6	-5.0
10462-11.1	328	123	0.39	111	9261	0.000014	64	0.02	140	0.115	1.8	13.119	1.6	0.4969	1.5	0.9819	0.1915	0.29	2601	33	2755	5	6.8
10462-3.1	260	85	0.34	82	8996	0.000050	31	0.09	118	0.094	2.2	13.934	1.7	0.5275	1.7	0.9800	0.1916	0.34	2731	37	2756	6	1.1
10462-26.1	338	118	0.36	61	10085	0.000027	94	0.05	152	0.101	1.9	13.859	1.7	0.5241	1.6	0.9792	0.1918	0.34	2717	36	2757	6	1.8
10462-3.2	561	240	0.44	91	10705	0.000039	42	0.07	248	0.109	2.4	13.596	1.5	0.5139	1.4	0.9855	0.1919	0.25	2673	31	2758	4	3.8
10462-14.1	887	16	0.02	74	11404	0.000017	16	0.03	421	0.005	4.8	14.608	1.6	0.5519	1.5	0.9497	0.1920	0.50	2833	35	2759	8	-3.3
10462-37.1	371	160	0.44	84	9182	0.000014	37	0.02	174	0.122	1.6	14.474	1.5	0.5467	1.4	0.9822	0.1920	0.28	2811	33	2760	5	-2.3
10462-13.1	1131	218	0.20	105	11437	0.000011	29	0.02	538	0.052	1.5	14.674	1.4	0.5536	1.4	0.9935	0.1923	0.16	2840	33	2762	3	-3.5
10462-44.1	717	168	0.24	161	10777	0.000003	249	0.01	342	0.069	1.6	14.736	1.5	0.5549	1.4	0.9845	0.1926	0.26	2845	33	2765	4	-3.6
10462-12.1	199	56	0.29	73	9078	0.000082	32	0.14	93	0.079	2.6	14.482	1.5	0.5446	1.5	0.9661	0.1929	0.40	2803	34	2767	7	-1.6
10462-24.1	421	236	0.58	88	9441	0.000017	18	0.03	194	0.164	1.3	14.273	1.7	0.5366	1.6	0.9699	0.1929	0.41	2769	37	2767	7	-0.1
10462-93.1	594	355	0.62	105	10786	0.000160	11	0.28	262	0.076	1.5	13.683	1.5	0.5140	1.4	0.9867	0.1931	0.24	2674	32	2768	4	4.2
10462-4.2	351	148	0.43	66	9876	0.000028	60	0.05	144	0.117	1.8	12.740	1.6	0.4772	1.6	0.9807	0.1936	0.32	2515	33	2773	5	11.2
10462-25.1	230	61	0.27	86	9124	0.000018	60	0.03	102	0.079	2.5	13.834	1.5	0.5175	1.5	0.9734	0.1939	0.34	2689	32	2775	6	3.8
10462-24.2	705	487	0.71	101	9935	0.000015	32	0.03	304	0.203	1.0	13.436	1.5	0.5015	1.5	0.9710	0.1943	0.36	2620	32	2779	6	6.9
10462-1.1	530	192	0.37	125	10386	0.000017	32	0.03	250	0.105	1.4	14.732	1.5	0.5493	1.4	0.9883	0.1945	0.22	2822	33	2781	4	-1.8
10462-35.1	370	97	0.27	122	10382	0.000011	24	0.02	170	0.076	2.0	14.383	1.5	0.5361	1.5	0.9843	0.1946	0.27	2767	34	2781	4	0.6
10462-30.1	465	302	0.67	122	9110	0.000047	52	0.08	214	0.151	1.2	14.386	1.5	0.5353	1.4	0.9820	0.1949	0.28	2764	33	2784	5	0.9
10462-56.1	294	137	0.48	74	9449	0.000050	17	0.09	127	0.126	1.9	13.467	1.5	0.5008	1.5	0.9764	0.1950	0.32	2617	32	2785	5	7.3
10462-16.1	367	134	0.38	113	9606	0.000035	128	0.06	165	0.104	1.7	14.117	1.5	0.5241	1.4	0.9662	0.1954	0.39	2717	32	2788	6	3.1
10462-4.1	465	256	0.57	117	9227	0.000008	58	0.01	211	0.157	1.3	14.230	1.5	0.5283	1.5	0.9854	0.1954	0.25	2734	33	2788	4	2.4
10462-8.1	210	93	0.46	47	8714	0.000037	66	0.06	97	0.125	2.0	14.442	1.6	0.5358	1.5	0.9710	0.1955	0.38	2766	34	2789	6	1.0
10462-16.2	533	293	0.57	72	9830	0.000005	48	0.01	237	0.161	1.2	14.003	1.5	0.5180	1.5	0.9873	0.1961	0.24	2691	33	2794	4	4.5
10462-42.1	245	207	0.87	112	7870	0.000011	222	0.02	111	0.246	1.4	14.353	1.5	0.5280	1.5	0.9703	0.1972	0.36	2733	33	2803	6	3.1
10462-84.1	66	28	0.45	172	8513	0.000162	58	0.28	30	0.120	5.5	14.995	1.8	0.5258	1.6	0.8845	0.2068	0.83	2724	35	2881	14	6.7
09SRB-D042A (GSC lab number z9974) IP540; NAD83: 65.67265N, -62.95977W																							
9974-64.1	376	187	0.51	nd	nd	0.000523	30	0.91	165	0.134	2.9	12.936	1.7	0.5099	1.2	0.7259	0.1840	1.15	2656	26	2689	19	1.5
9974-22.1	295	290	1.01	nd	nd	0.000130	21	0.23	143	0.279	1.4	14.294	1.2	0.5632	1.1	0.9502	0.1841	0.37	2880	26	2690	6	-8.8
9974-176.1	290	185	0.66	nd	nd	0.000151	64	0.26	125	0.178	2.3	12.789	1.4	0.5019	1.2	0.8426	0.1848	0.77	2622	26	2696	13	3.4
9974-197.2	735	420	0.59	nd	nd	0.000048	22	0.08	348	0.162	1.2	14.041	1.1	0.5507	1.1	0.9795	0.1849	0.22	2828	24	2698	4	-6.0
9974-109.1	191	215	1.16	nd	nd	0.000193	22	0.33	92	0.313	1.6	14.280	1.3	0.5588	1.2	0.9243	0.1854	0.49	2861	27	2701	8	-7.3
9974-197.1	703	459	0.68	nd	nd	0.000127	17	0.22	318	0.186	1.4	13.479	1.1	0.5264	1.1	0.9629	0.1857	0.31	2726	24	2705	5	-1.0
9974-196.1	646	265	0.42	nd	nd	0.000156	21	0.27	294	0.115	1.8	13.604	1.2	0.5305	1.1	0.9523	0.1860	0.35	2743	25	2707	6	-1.6
9974-163.2	167	167	1.03	nd	nd	0.000629	23	1.09	69	0.277	2.9	12.370	1.8	0.4822	1.3	0.7601	0.1861	1.14	2537	28	2708	19	7.6
9974-167.1	488	423	0.90	nd	nd	0.000191	19	0.33	217	0.243	1.5	13.344	1.2	0.5185	1.1	0.9413	0.1866	0.40	2693	25	2713	7	0.9
9974-167.2	423	414	1.01	nd	nd	0.000120	36	0.21	173	0.279	1.2	12.331	1.2	0.4778	1.1	0.9258	0.1872	0.44	2518	23	2718	7	8.9
9974-158.1	156	164	1.08	nd	nd	0.000617	21	1.07	70	0.313	2.1	13.451	1.8	0.5204	1.3	0.7655	0.1875	1.13	2701	30	2720	19	0.9
9974-100.1	211	267	1.31	nd	nd	0.000736	15	1.28	91	0.369	2.4	13.079	1.6	0.5051	1.3	0.8198	0.1878	0.92	2636	29	2723	15	3.9
9974-190.1	184	157	0.88	nd	nd	0.000680	14	1.18	84	0.237	2.3	13.836	1.6	0.5311	1.3	0.8042	0.1889	0.97	2746	29	2733	16	-0.6
9974-172.1	305	228	0.77	nd	nd	0.000440	21	0.76	138	0.205	1.8	13.722	1.4	0.5255	1.2	0.8595	0.1894	0.70	2723	26	2737	12	0.6
9974-161.2	745	143	0.20	nd	nd	0.000080	16	0.14	361	0.054	1.8	14.744	1.1	0.5643	1.0	0.9685	0.1895	0.27	2884	24	2738	4	-6.6
9974-19.1	272	71	0.27	nd	nd	0.000077	26	0.13	122	0.071	2.6	13.667	1.2	0.5230	1.1	0.9577	0.1895	0.33	2712	25	2738	5	1.2

Table 1. Continued.

Spot name	U (ppm)	Th (ppm)	$\frac{Th}{U}$	Yb (ppm)	Hf (ppm)	$\frac{^{204}Pb}{^{206}Pb}$	% ±	$f(206)^{204}$ %	$^{206}Pb^*$ (ppm)	$\frac{^{208*}Pb}{^{206*}Pb}$	% ±	$\frac{^{207*}Pb}{^{235}U}$	% ±	$\frac{^{206*}Pb}{^{238}U}$	% ±	Corr Coeff	$\frac{^{207*}Pb}{^{206*}Pb}$	% ±	Apparent ages (Ma) $\frac{^{206}Pb}{^{238}U}$	$\pm\frac{^{206}Pb}{^{238}U}$	$\frac{^{207}Pb}{^{206}Pb}$	$\pm\frac{^{207}Pb}{^{206}Pb}$	Disc. (%)
09SRB-D042A (GSC lab number z9974) IP540; NAD83: 65.67265N, -62.95977W (continued)																							
9974-175.1	295	70	0.25	nd	nd	0.000284	20	0.49	132	0.065	3.3	13.705	1.3	0.5226	1.2	0.9099	0.1902	0.54	2710	26	2744	9	1.5
9974-87.1	309	81	0.27	nd	nd	0.000508	16	0.88	140	0.070	4.2	13.842	1.4	0.5275	1.2	0.8668	0.1903	0.70	2731	27	2745	12	0.6
9974-188.1	323	132	0.42	nd	nd	0.000247	19	0.43	143	0.108	2.6	13.562	1.3	0.5157	1.2	0.9219	0.1907	0.50	2681	26	2748	8	3.0
9974-57.1	494	124	0.26	nd	nd	0.000397	13	0.69	223	0.067	3.3	13.786	1.3	0.5242	1.1	0.8938	0.1908	0.57	2717	25	2749	9	1.4
9974-163.1	438	135	0.32	nd	nd	0.000302	23	0.52	198	0.095	3.2	13.848	1.4	0.5263	1.2	0.8617	0.1908	0.69	2726	26	2749	11	1.1
9974-201.1	795	91	0.12	nd	nd	0.000266	11	0.46	373	0.031	2.7	14.390	1.3	0.5461	1.3	0.9754	0.1911	0.30	2809	30	2752	5	-2.6
9974-183.1	682	114	0.17	nd	nd	0.000152	23	0.26	315	0.047	3.2	14.197	1.1	0.5379	1.1	0.9525	0.1914	0.35	2774	24	2755	6	-0.9
9974-198.2	611	247	0.42	nd	nd	0.000206	30	0.36	290	0.101	2.5	14.606	1.2	0.5527	1.1	0.9136	0.1917	0.49	2837	25	2756	8	-3.6
9974-170.1	403	57	0.15	nd	nd	0.000207	23	0.36	186	0.039	3.4	14.249	1.4	0.5383	1.1	0.7953	0.1920	0.87	2776	26	2759	14	-0.8
9974-12.1	407	137	0.35	nd	nd	0.000364	15	0.63	186	0.088	3.4	14.069	1.3	0.5315	1.2	0.9113	0.1920	0.53	2748	26	2759	9	0.5
9974-193.1	344	108	0.33	nd	nd	0.000529	12	0.92	157	0.083	2.5	14.080	1.3	0.5318	1.2	0.9085	0.1920	0.53	2749	26	2760	9	0.5
9974-163.3	422	141	0.35	nd	nd	0.000016	47	0.03	166	0.096	2.2	12.139	1.1	0.4580	1.1	0.9653	0.1922	0.30	2431	22	2761	5	14.3
9974-181.1	226	213	0.97	nd	nd	0.000753	18	1.31	104	0.248	2.4	14.142	1.8	0.5335	1.2	0.6939	0.1922	1.27	2756	27	2761	21	0.2
9974-182.1	121	84	0.71	nd	nd	0.001074	14	1.86	53	0.202	2.8	13.522	1.8	0.5097	1.4	0.7829	0.1924	1.14	2655	31	2763	19	4.8
9974-198.1	303	218	0.74	nd	nd	0.000315	18	0.55	138	0.211	2.4	14.118	1.3	0.5315	1.2	0.9091	0.1926	0.54	2748	26	2765	9	0.7
9974-202.1	434	94	0.22	nd	nd	0.000167	29	0.29	200	0.062	2.9	14.307	1.2	0.5377	1.1	0.9302	0.1930	0.44	2774	25	2768	7	-0.3
9974-171.1	333	98	0.30	nd	nd	0.000223	36	0.39	152	0.081	2.9	14.213	1.3	0.5336	1.2	0.8830	0.1932	0.63	2757	26	2769	10	0.6
9974-203.1	374	60	0.17	nd	nd	0.000425	26	0.74	171	0.044	4.3	14.197	1.4	0.5329	1.2	0.8287	0.1932	0.78	2754	26	2770	13	0.7
9974-176.2	600	1085	1.87	nd	nd	0.000028	135	0.05	292	0.527	0.7	15.094	1.1	0.5666	1.1	0.9568	0.1932	0.32	2894	25	2770	5	-5.6
9974-57.2	159	129	0.84	nd	nd	0.000677	20	1.17	71	0.220	3.8	13.798	1.8	0.5170	1.4	0.7925	0.1936	1.08	2687	31	2773	18	3.8
9974-159.1	581	60	0.11	nd	nd	0.000288	17	0.50	271	0.028	6.9	14.500	1.5	0.5433	1.1	0.7366	0.1936	1.01	2797	25	2773	16	-1.1
9974-183.2	250	270	1.11	nd	nd	0.000203	41	0.35	117	0.313	2.2	14.471	1.5	0.5421	1.2	0.8369	0.1936	0.80	2792	28	2773	13	-0.9
9974-179.1	206	135	0.68	nd	nd	0.000080	47	0.14	95	0.172	2.1	14.340	1.3	0.5354	1.2	0.9374	0.1942	0.44	2764	27	2778	7	0.6
9974-166.1	200	104	0.54	nd	nd	0.000572	16	0.99	89	0.150	2.7	13.924	1.5	0.5198	1.3	0.8597	0.1943	0.75	2698	28	2779	12	3.5
9974-186.1	211	227	1.11	nd	nd	0.000266	38	0.46	96	0.312	2.0	14.420	2.7	0.5312	2.6	0.9564	0.1969	0.78	2747	57	2800	13	2.4
9974-161.1	148	205	1.43	nd	nd	0.000232	60	0.40	69	0.414	2.1	14.831	1.7	0.5406	1.4	0.7884	0.1990	1.07	2786	31	2818	17	1.4
09SRB-D040B (GSC lab number z9973) IP540; NAD83: 65.68733N, -62.96395W																							
9973-87.1	1985	152	0.08	nd	nd	0.000028	30	0.05	893	0.022	3.0	13.190	1.1	0.5236	1.1	0.9829	0.1827	0.20	2714	24	2678	3	-1.7
9973-101.2	879	675	0.79	nd	nd	0.000088	17	0.15	401	0.221	0.9	13.405	1.1	0.5309	1.1	0.9637	0.1831	0.30	2745	24	2681	5	-2.9
9973-59.1	1526	777	0.53	nd	nd	0.000114	16	0.20	690	0.148	0.9	13.294	1.1	0.5264	1.1	0.9824	0.1832	0.20	2726	24	2682	3	-2.0
9973-84.1	993	792	0.82	nd	nd	0.000046	32	0.08	441	0.227	1.0	13.076	1.1	0.5165	1.1	0.9774	0.1836	0.23	2684	23	2686	4	0.1
9973-70.1	893	599	0.69	nd	nd	0.000232	10	0.40	397	0.188	1.1	13.121	1.1	0.5179	1.1	0.9700	0.1837	0.26	2690	23	2687	4	-0.2
9973-42.1	954	226	0.24	nd	nd	0.000177	18	0.31	457	0.060	2.6	14.137	1.2	0.5577	1.1	0.9437	0.1838	0.40	2857	26	2688	7	-7.8
9973-99.1	980	659	0.69	nd	nd	0.000170	11	0.29	442	0.193	1.0	13.318	1.1	0.5248	1.0	0.9768	0.1841	0.23	2719	23	2690	4	-1.3
9973-65.1	975	533	0.56	nd	nd	0.000094	18	0.16	432	0.154	1.3	13.116	1.1	0.5159	1.1	0.9742	0.1844	0.25	2682	23	2693	4	0.5
9973-73.1	744	449	0.62	nd	nd	0.000186	13	0.32	335	0.184	1.7	13.357	1.1	0.5243	1.1	0.9661	0.1847	0.29	2718	24	2696	5	-1.0
9973-78.1	1236	1128	0.94	nd	nd	0.000030	68	0.05	554	0.260	0.8	13.289	1.1	0.5214	1.0	0.9763	0.1849	0.23	2705	23	2697	4	-0.4
9973-107.1	1020	842	0.85	nd	nd	0.000054	17	0.09	462	0.235	0.8	13.446	1.1	0.5273	1.0	0.9851	0.1849	0.18	2730	23	2698	3	-1.5
9973-104.3	1058	701	0.68	nd	nd	0.000031	23	0.05	419	0.183	1.0	11.798	1.1	0.4616	1.1	0.9679	0.1854	0.28	2447	22	2702	5	11.3
9973-108.1	997	596	0.62	nd	nd	0.000077	21	0.13	450	0.172	0.9	13.449	1.1	0.5259	1.0	0.9828	0.1855	0.19	2724	23	2703	3	-1.0
9973-104.1	983	675	0.71	nd	nd	0.000048	22	0.08	437	0.195	1.0	13.250	1.1	0.5175	1.1	0.9810	0.1857	0.21	2689	23	2704	3	0.7
9973-78.2	1065	759	0.74	nd	nd	0.000031	26	0.05	436	0.205	1.0	12.208	1.1	0.4766	1.0	0.9822	0.1858	0.20	2513	22	2705	3	8.6
9973-104.2	918	644	0.72	nd	nd	0.000050	24	0.09	369	0.196	1.0	11.980	1.1	0.4676	1.1	0.9639	0.1858	0.30	2473	22	2706	5	10.3
9973-81.1	620	295	0.49	nd	nd	0.000872	6	1.51	278	0.133	1.4	13.401	1.2	0.5226	1.1	0.9134	0.1860	0.48	2710	24	2707	8	-0.1

Notes (*see* Stern, 1997):
Spot name follows the convention x-y.z; where x = sample number, y = grain number, and z = spot number. Multiple analyses in an individual spot are labelled as x-y.z.z
Uncertainties reported at 1s and are calculated by using SQUID 2.23.08.10.21, rev. 21 Oct 2008
nd = not determined
$f206^{204}$ refers to mole percent of total ^{206}Pb that is due to common Pb, calculated using the ^{204}Pb-method; common Pb composition used is the surface blank (4/6: 0.05770; 7/6: 0.89500; 8/6: 2.13840)
* refers to radiogenic Pb (corrected for common Pb)
Discordance relative to origin = 100 * ((207/206 age -206/238 age)/($^{207}Pb/^{206}Pb$ age))
Calibration standard 6266; U = 910 ppm; Age = 559 Ma; $^{206}Pb/^{238}U$ = 0.09059
Analytical details
IP540: 23 µm spot; analyses marked with * analysed using 16 µm spot; 5 scans; U-Pb calibration error 1.0% (included);
Measured age of secondary standard 1242 = 2680 ± 6 Ma (n = 12); no mass fractionation correction.
IP604: 23 µm spot; 6 scans; U-Pb calibration error 1.41% (included);
Measured age of secondary standard 1242 = 2679 ± 4 Ma (n = 21); no mass fractionation correction.

Table 1. Continued.

Spot name	U (ppm)	Th (ppm)	Th/U	Yb (ppm)	Hf (ppm)	$^{204}Pb/^{206}Pb$	% ±	$f(206)^{204}$ %	$^{206}Pb^*$ (ppm)	$^{208*}Pb/^{206*}Pb$	% ±	$^{207*}Pb/^{235}U$	% ±	$^{206*}Pb/^{238}U$	% ±	Corr Coeff	$^{207*}Pb/^{206*}Pb$	% ±	Apparent ages (Ma) $^{206}Pb/^{238}U$	$\pm ^{206}Pb/^{238}U$	$^{207}Pb/^{206}Pb$	$\pm ^{207}Pb/^{206}Pb$	Disc. (%)
09SRB-D040B (GSC lab number z9973) IP540; NAD83: 65.68733N, -62.96395W (continued)																							
9973-101.1	883	552	0.65	nd	nd	0.000091	20	0.16	390	0.181	1.4	13.182	1.1	0.5139	1.1	0.9728	0.1860	0.25	2673	23	2707	4	1.5
9973-79.2	1140	116	0.11	nd	nd	0.000154	13	0.27	549	0.028	3.4	14.502	1.1	0.5605	1.1	0.9527	0.1876	0.34	2869	25	2722	6	-6.7
9973-63.1	383	128	0.34	nd	nd	0.000552	11	0.96	174	0.083	2.4	13.670	1.2	0.5278	1.1	0.9110	0.1878	0.51	2732	25	2723	8	-0.4
9973-41.1	1193	109	0.09	nd	nd	0.000185	11	0.32	550	0.019	3.7	13.904	1.1	0.5365	1.1	0.9716	0.1880	0.26	2769	24	2724	4	-2.0
9973-21.1	2329	658	0.29	nd	nd	0.000038	18	0.07	1206	0.091	1.4	15.665	1.1	0.6028	1.1	0.9814	0.1885	0.21	3041	26	2729	3	-14.4
9973-91.1	1567	84	0.06	nd	nd	0.000016	49	0.03	733	0.015	4.2	14.229	1.1	0.5449	1.0	0.9354	0.1894	0.39	2804	24	2737	6	-3.0
9973-57.1	270	116	0.45	nd	nd	0.000479	13	0.83	123	0.108	3.5	13.867	1.4	0.5305	1.2	0.8638	0.1896	0.70	2744	27	2738	11	-0.2
9973-106.1	568	198	0.36	nd	nd	0.000063	41	0.11	259	0.100	1.8	13.927	1.1	0.5304	1.1	0.9641	0.1904	0.30	2743	24	2746	5	0.1
9973-9.1	882	60	0.07	nd	nd	0.000024	49	0.04	399	0.021	2.9	13.807	1.1	0.5258	1.0	0.9819	0.1904	0.20	2724	23	2746	3	1.0
9973-61.1	1059	73	0.07	nd	nd	0.000111	17	0.19	490	0.019	4.2	14.189	1.1	0.5389	1.1	0.9718	0.1910	0.26	2779	24	2750	4	-1.3
9973-67.1	930	36	0.04	nd	nd	0.000074	25	0.13	427	0.011	4.2	14.094	1.1	0.5351	1.1	0.9748	0.1910	0.24	2763	24	2751	4	-0.5
9973-66.1	260	123	0.49	nd	nd	0.000434	15	0.75	119	0.134	2.3	14.067	1.4	0.5323	1.2	0.8636	0.1917	0.69	2751	27	2756	11	0.2
9973-72.1	763	46	0.06	nd	nd	0.000126	18	0.22	344	0.016	5.1	13.870	1.1	0.5238	1.1	0.9640	0.1920	0.30	2715	24	2760	5	2.0
9973-42.2	271	117	0.45	nd	nd	0.000394	20	0.68	116	0.123	3.7	13.229	1.6	0.4987	1.2	0.8000	0.1924	0.93	2608	27	2763	15	6.8
9973-41.2	343	142	0.43	nd	nd	0.000273	18	0.47	160	0.106	2.4	14.356	1.2	0.5411	1.1	0.9246	0.1924	0.47	2788	26	2763	8	-1.1
9973-21.2	382	85	0.23	nd	nd	0.000399	31	0.69	170	0.053	6.0	13.747	1.5	0.5171	1.2	0.8064	0.1928	0.87	2687	26	2766	14	3.5
9973-39.1	468	174	0.38	nd	nd	0.000111	25	0.19	210	0.110	2.1	13.863	1.2	0.5213	1.1	0.9547	0.1929	0.35	2705	25	2767	6	2.7
9973-85.1	331	192	0.60	nd	nd	0.000429	12	0.74	153	0.155	2.6	14.294	1.3	0.5372	1.1	0.8984	0.1930	0.56	2772	26	2768	9	-0.2
9973-29.1	368	148	0.42	nd	nd	0.000316	17	0.55	170	0.113	3.1	14.341	1.3	0.5365	1.2	0.9156	0.1939	0.52	2769	27	2775	8	0.3
9973-103.1	1111	785	0.73	nd	nd	0.000035	24	0.06	522	0.201	0.9	14.651	1.1	0.5477	1.1	0.9854	0.1940	0.18	2816	24	2776	3	-1.7
9973-97.1	798	354	0.46	nd	nd	0.000181	11	0.31	371	0.126	1.3	14.515	1.1	0.5411	1.1	0.9620	0.1946	0.30	2788	24	2781	5	-0.3
9973-79.1	267	105	0.40	nd	nd	0.000282	20	0.49	124	0.119	3.4	14.483	1.3	0.5389	1.2	0.9074	0.1949	0.56	2779	27	2784	9	0.2
9973-61.2	251	103	0.43	nd	nd	0.000322	35	0.56	118	0.128	3.6	14.750	1.6	0.5470	1.3	0.7959	0.1956	0.96	2813	29	2790	16	-1.0
9973-72.2	246	98	0.41	nd	nd	0.000235	65	0.41	111	0.115	3.8	14.089	1.7	0.5223	1.3	0.7678	0.1956	1.06	2709	28	2790	17	3.6
9973-58.1	318	116	0.38	nd	nd	0.000118	29	0.21	144	0.111	2.5	14.264	1.2	0.5277	1.2	0.9391	0.1961	0.43	2732	26	2794	7	2.7
9973-102.1	136	43	0.33	nd	nd	0.000352	23	0.61	63	0.086	4.7	15.205	1.5	0.5375	1.3	0.8799	0.2052	0.70	2773	29	2868	11	4.1
9973-93.1	149	98	0.68	nd	nd	0.000404	20	0.70	68	0.174	3.9	15.158	1.5	0.5333	1.3	0.8845	0.2061	0.69	2756	29	2875	11	5.1
9973-96.1	87	28	0.33	nd	nd	0.000487	31	0.84	42	0.084	6.4	16.968	1.9	0.5604	1.5	0.7833	0.2196	1.15	2868	34	2978	19	4.5
07SAB-02 (GSC lab number z10151) IP561_3; NAD83: 66.32667N, -65.50183W																							
10151-37.1	681	403	0.61	nd	nd	0.000035	25	0.06	194	0.178	1.1	5.160	1.1	0.3320	1.1	0.9673	0.1127	0.28	1848	17	1844	5	-0.2
10151-19.1	592	315	0.55	nd	nd	0.000019	50	0.03	168	0.163	1.2	5.140	1.1	0.3307	1.0	0.9596	0.1128	0.30	1842	16	1844	5	0.2
10151-13.1	247	143	0.60	nd	nd	0.000019	84	0.03	70	0.177	1.8	5.123	1.2	0.3290	1.1	0.8848	0.1130	0.55	1833	17	1847	10	0.9
10151-44.1	523	231	0.46	nd	nd	0.000008	85	0.01	149	0.134	1.4	5.205	1.1	0.3325	1.0	0.9197	0.1135	0.44	1851	17	1857	8	0.4
10151-11.1	613	281	0.47	nd	nd	0.000040	31	0.07	172	0.136	1.2	5.120	1.1	0.3270	1.0	0.9593	0.1135	0.30	1824	16	1857	5	2.0
10151-38.1	496	261	0.54	nd	nd	-0.000005	284	-0.01	141	0.160	1.3	5.198	1.1	0.3318	1.0	0.9462	0.1136	0.35	1847	17	1858	6	0.7
10151-88.2	478	250	0.54	nd	nd	0.000011	45	0.02	134	0.158	1.3	5.104	1.1	0.3254	1.0	0.9580	0.1137	0.31	1816	16	1860	6	2.7
10151-42.1	247	141	0.59	nd	nd	0.000068	98	0.12	70	0.170	1.8	5.207	1.5	0.3317	1.2	0.8024	0.1138	0.90	1847	19	1862	16	0.9
10151-109.1	177	67	0.39	nd	nd	0.000042	88	0.07	50	0.114	2.6	5.140	1.3	0.3275	1.1	0.8485	0.1138	0.67	1826	17	1862	12	2.2
10151-20.1	347	190	0.57	nd	nd	0.000038	53	0.07	99	0.167	2.3	5.202	1.1	0.3310	1.0	0.9251	0.1140	0.43	1843	17	1864	8	1.3
10151-114.2	743	121	0.17	nd	nd	0.000025	25	0.04	212	0.050	1.9	5.233	1.1	0.3328	1.0	0.9724	0.1141	0.25	1852	17	1865	5	0.8
10151-22.1	199	68	0.35	nd	nd	0.000041	87	0.07	56	0.104	2.6	5.175	1.2	0.3289	1.1	0.8579	0.1141	0.64	1833	17	1866	12	2.1
10151-94.2	641	209	0.34	nd	nd	0.000025	20	0.04	180	0.095	1.5	5.163	1.1	0.3278	1.0	0.9677	0.1142	0.27	1828	16	1868	5	2.5
10151-67.1	217	97	0.46	nd	nd	0.000021	119	0.04	62	0.132	2.2	5.256	1.2	0.3321	1.1	0.8900	0.1148	0.54	1848	17	1877	10	1.7
10151-14.1	380	209	0.57	nd	nd	0.000011	61	0.02	109	0.171	1.5	5.313	1.1	0.3355	1.0	0.9473	0.1149	0.35	1865	17	1878	6	0.8
10151-54.1	221	89	0.41	nd	nd	0.000037	51	0.06	63	0.121	2.3	5.310	1.2	0.3350	1.1	0.9053	0.1149	0.50	1863	17	1879	9	1.0
10151-99.1	198	76	0.40	nd	nd	0.000050	27	0.09	56	0.114	2.4	5.218	1.2	0.3289	1.1	0.9068	0.1151	0.50	1833	17	1881	9	2.9
10151-114.1	176	74	0.43	nd	nd	0.000049	32	0.08	50	0.127	2.4	5.244	1.2	0.3302	1.1	0.8998	0.1152	0.52	1839	17	1883	9	2.7
10151-45.1	180	71	0.41	nd	nd	0.000033	98	0.06	51	0.127	2.4	5.258	1.2	0.3310	1.1	0.8651	0.1152	0.62	1843	17	1883	11	2.4
10151-9.1	225	92	0.42	nd	nd	0.000040	126	0.07	65	0.124	2.1	5.327	1.3	0.3351	1.1	0.8247	0.1153	0.73	1863	17	1884	13	1.3
10151-94.1	182	60	0.34	nd	nd	0.000023	78	0.04	52	0.101	2.7	5.327	1.2	0.3350	1.1	0.8934	0.1153	0.54	1863	17	1885	10	1.3
10151-15.1	1387	314	0.23	nd	nd	0.000006	86	0.01	412	0.070	1.2	5.498	1.0	0.3455	1.0	0.9663	0.1154	0.27	1913	17	1886	5	-1.6
10151-88.1	187	95	0.53	nd	nd	0.000001	89	0.00	53	0.154	3.8	5.253	1.2	0.3299	1.1	0.9153	0.1155	0.47	1838	17	1887	8	3.0
10151-21.1	310	155	0.52	nd	nd	0.000038	34	0.07	90	0.156	1.7	5.408	1.1	0.3393	1.0	0.9336	0.1156	0.40	1883	17	1889	7	0.4

Table 1. Continued.

Spot name	U (ppm)	Th (ppm)	Th/U	Yb (ppm)	Hf (ppm)	$^{204}Pb/^{206}Pb$	% ±	$f(206)^{204}$ %	$^{206}Pb^*$ (ppm)	$^{208*}Pb/^{206*}Pb$	% ±	$^{207*}Pb/^{235}U$	% ±	$^{206*}Pb/^{238}U$	% ±	Corr Coeff	$^{207*}Pb/^{206*}Pb$	% ±	Apparent ages (Ma) $^{206}Pb/^{238}U$	$\pm^{206}Pb/^{238}U$	$^{207}Pb/^{206}Pb$	$\pm^{207}Pb/^{206}Pb$	Disc. (%)
07SAB-02 (GSC lab number z10151) IP561_3; NAD83: 66.32667N, -65.50183W (continued)																							
10151-5.1	220	109	0.51	nd	nd	0.000062	28	0.11	63	0.145	2.1	5.351	1.2	0.3354	1.1	0.9077	0.1157	0.49	1865	17	1891	9	1.6
10151-41.1	486	320	0.68	nd	nd	0.000013	13	0.02	141	0.197	1.2	5.406	1.1	0.3388	1.0	0.9600	0.1157	0.30	1881	17	1891	5	0.7
10151-116.1	180	72	0.41	nd	nd	0.000015	30	0.03	52	0.123	2.4	5.386	1.2	0.3371	1.1	0.9148	0.1159	0.49	1873	18	1894	9	1.3
10151-10.1	1007	297	0.30	nd	nd	0.000000	540	0.00	300	0.088	1.2	5.561	1.1	0.3473	1.1	0.9811	0.1162	0.21	1921	18	1898	4	-1.4
10151-46.1	214	89	0.43	nd	nd	0.000003	501	0.01	61	0.132	2.2	5.363	1.2	0.3340	1.1	0.9110	0.1164	0.48	1858	17	1902	9	2.7
10151-8.1	523	366	0.72	nd	nd	0.000014	44	0.02	154	0.211	1.1	5.502	1.1	0.3424	1.1	0.9661	0.1166	0.29	1898	18	1904	5	0.4
10151-17.1	360	156	0.45	nd	nd	-0.000003	817	-0.01	106	0.133	1.7	5.528	1.2	0.3430	1.1	0.9213	0.1169	0.47	1901	18	1909	8	0.5
10151-12.1	273	149	0.57	nd	nd	0.000001	8	0.00	81	0.170	1.7	5.614	1.1	0.3452	1.0	0.9374	0.1180	0.39	1912	17	1926	7	0.8
09SRB-M109A (GSC lab number z10150) IP561_4; NAD83: 66.40735N, -64.86038W																							
10150-29.1	250	71	0.29	297	11923	0.000039	30	0.07	71	0.085	2.2	5.193	1.44	0.3325	1.4	0.9640	0.1133	0.38	1850	22	1853	7	0.2
10150-46.1	192	69	0.37	173	10211	0.000022	161	0.04	54	0.112	2.0	5.132	1.49	0.3271	1.4	0.9296	0.1138	0.55	1824	22	1861	10	2.3
10150-55.1	303	86	0.29	387	11877	0.000058	24	0.10	86	0.084	2.0	5.169	1.43	0.3291	1.4	0.9671	0.1139	0.36	1834	22	1863	7	1.8
10150-30.1	292	97	0.34	266	11564	0.000041	22	0.07	82	0.102	1.9	5.149	1.41	0.3269	1.4	0.9706	0.1142	0.34	1823	22	1868	6	2.7
10150-29.2	291	94	0.33	294	11622	0.000020	99	0.04	83	0.100	1.7	5.210	1.43	0.3302	1.4	0.9631	0.1144	0.38	1840	22	1871	7	1.9
10150-79.1	292	88	0.31	280	11823	0.000020	24	0.04	83	0.092	1.9	5.241	1.41	0.3306	1.4	0.9742	0.1150	0.32	1841	22	1879	6	2.3
10150-84.1	188	71	0.39	455	11195	-0.000005	84	-0.01	54	0.120	1.9	5.285	1.45	0.3333	1.4	0.9679	0.1150	0.36	1854	23	1880	7	1.6
10150-86.1	372	100	0.28	324	11791	0.000017	103	0.03	106	0.082	1.8	5.266	1.42	0.3318	1.4	0.9709	0.1151	0.34	1847	22	1882	6	2.1
10150-80.1	359	120	0.34	298	11688	0.000025	33	0.04	104	0.100	1.6	5.370	1.40	0.3383	1.4	0.9785	0.1151	0.29	1878	22	1882	5	0.2
10150-44.1	503	143	0.29	375	11885	0.000003	99	0.00	144	0.089	1.4	5.299	1.39	0.3335	1.4	0.9856	0.1152	0.24	1855	22	1883	4	1.7
10150-82.1	153	45	0.30	420	11712	0.000047	77	0.08	44	0.090	2.7	5.363	1.53	0.3373	1.4	0.9155	0.1153	0.62	1874	23	1885	11	0.7
10150-7.1	384	100	0.27	480	12036	0.000013	48	0.02	111	0.078	1.8	5.346	1.42	0.3360	1.4	0.9790	0.1154	0.29	1867	23	1886	5	1.2
10150-56.1	569	186	0.34	386	11652	-0.000002	422	0.00	165	0.102	1.3	5.369	1.39	0.3375	1.4	0.9858	0.1154	0.23	1874	22	1886	4	0.7
10150-81.1	715	416	0.60	549	11656	0.000007	80	0.01	214	0.181	0.9	5.561	1.39	0.3493	1.4	0.9871	0.1155	0.22	1931	23	1887	4	-2.7
10150-32.1	787	93	0.12	488	12882	0.000000	2418	0.00	228	0.034	1.8	5.377	1.38	0.3374	1.4	0.9879	0.1156	0.21	1874	22	1889	4	0.9
10150-5.1	348	90	0.27	307	12082	-0.000005	151	-0.01	100	0.080	1.8	5.337	1.40	0.3349	1.4	0.9781	0.1156	0.29	1862	22	1889	5	1.6
10150-57.1	259	74	0.30	269	11965	0.000010	136	0.02	75	0.089	2.1	5.352	1.42	0.3358	1.4	0.9666	0.1156	0.36	1866	22	1889	7	1.4
10150-8.1	438	118	0.28	337	11985	0.000017	62	0.03	126	0.084	1.6	5.352	1.41	0.3355	1.4	0.9809	0.1157	0.27	1865	22	1891	5	1.5
10150-66.1	521	153	0.30	407	11951	0.000001	76	0.00	146	0.093	1.4	5.194	1.39	0.3256	1.4	0.9863	0.1157	0.23	1817	22	1891	4	4.5
10150-54.1	277	107	0.40	314	11316	0.000018	102	0.03	79	0.119	1.7	5.321	1.46	0.3334	1.4	0.9657	0.1157	0.38	1855	23	1891	7	2.2
10150-83.1	445	124	0.29	327	12070	0.000008	132	0.01	129	0.084	1.5	5.382	1.43	0.3369	1.4	0.9589	0.1159	0.41	1872	22	1893	7	1.3
10150-4.1	442	140	0.33	386	11770	0.000017	53	0.03	129	0.099	1.4	5.406	1.39	0.3383	1.4	0.9817	0.1159	0.27	1879	22	1894	5	0.9
10150-5.2	449	130	0.30	336	11906	-0.000008	150	-0.01	125	0.089	1.5	5.195	1.41	0.3251	1.4	0.9807	0.1159	0.28	1814	22	1894	5	4.8
10150-30.2	360	122	0.35	287	11469	0.000019	28	0.03	102	0.106	1.6	5.303	1.47	0.3318	1.4	0.9807	0.1159	0.29	1847	23	1894	5	2.9
10150-46.3	264	97	0.38	240	9979	0.000010	117	0.02	81	0.113	1.8	5.686	1.42	0.3552	1.4	0.9695	0.1161	0.35	1959	23	1897	6	-3.8
10150-85.1	356	79	0.23	298	12283	0.000014	26	0.02	102	0.069	1.9	5.350	1.51	0.3341	1.4	0.9591	0.1161	0.43	1858	23	1898	8	2.4
10150-1.1	429	140	0.34	397	10616	0.000001	1107	0.00	121	0.099	1.5	5.262	1.41	0.3286	1.4	0.9749	0.1161	0.31	1831	22	1898	6	4.0
10150-31.1	512	160	0.32	358	12061	0.000003	98	0.00	149	0.094	1.5	5.427	1.39	0.3389	1.4	0.9838	0.1162	0.25	1881	22	1898	4	1.0
10150-46.2	321	17	0.05	182	12607	-0.000018	48	-0.03	99	0.019	4.2	5.850	1.43	0.3580	1.4	0.9754	0.1185	0.32	1973	24	1934	6	-2.3
10150-55.3	345	149	0.45	420	10227	0.000005	413	0.01	98	0.135	1.4	5.410	1.45	0.3287	1.4	0.9694	0.1194	0.36	1832	22	1947	6	6.7
10150-55.2	422	232	0.57	465	8974	0.000014	38	0.02	123	0.162	1.4	5.679	1.40	0.3394	1.4	0.9837	0.1214	0.25	1884	22	1976	4	5.4
10150-20.1	276	122	0.46	224	10345	-0.000001	650	0.00	99	0.131	1.4	8.030	1.62	0.4162	1.4	0.8776	0.1399	0.78	2243	27	2226	13	-0.9

Notes (*see* Stern, 1997):
Spot name follows the convention x-y.z; where x = sample number, y = grain number, and z = spot number. Multiple analyses in an individual spot are labelled as x-y.z.z
Uncertainties reported at 1s and are calculated by using SQUID 2.23.08.10.21, rev. 21 Oct 2008
nd = not determined
$f206^{204}$ refers to mole percent of total ^{206}Pb that is due to common Pb, calculated using the ^{204}Pb-method; common Pb composition used is the surface blank (4/6: 0.05770; 7/6: 0.89500; 8/6: 2.13840)
* refers to radiogenic Pb (corrected for common Pb)
Discordance relative to origin = 100 * ((207/206 age -206/238 age)/($^{207}Pb/^{206}Pb$ age))
Calibration standard 6266; U = 910 ppm; Age = 559 Ma; $^{206}Pb/^{238}U = 0.09059$
Analytical details
IP540: 23 µm spot; analyses marked with * analysed using 16 µm spot; 5 scans; U-Pb calibration error 1.0% (included);
Measured age of secondary standard 1242 = 2680 ± 6 Ma (n = 12); no mass fractionation correction.
IP561_3: 23 µm spot;. 6 scans; U-Pb calibration error 1.0% (included);
Measured age of secondary standard 1242 = 2679 ± 3 Ma (n = 21); no mass fractionation correction.
IP561_4: 23 µm spot;. 6 scans; U-Pb calibration error 1.36% (included);
Measured age of secondary standard 1242 = 2677 ± 4 Ma (n = 15); Intraelement mass fractionation correction of 0.13% applied to unknowns.

Table 1. Continued.

Spot name	U (ppm)	Th (ppm)	Th/U	Yb (ppm)	Hf (ppm)	$^{204}Pb/^{206}Pb$	% ±	$f(206)^{204}$ %	$^{206}Pb^*$ (ppm)	$^{208*}Pb/^{206*}Pb$	% ±	$^{207*}Pb/^{235}U$	% ±	$^{206*}Pb/^{238}U$	% ±	Corr Coeff	$^{207*}Pb/^{206*}Pb$	% ±	Apparent ages (Ma) $^{206}Pb/^{238}U$	$\pm ^{206}Pb/^{238}U$	$^{207}Pb/^{206}Pb$	$\pm ^{207}Pb/^{206}Pb$	Disc. (%)
09SRB-D010C (GSC lab number z9972) IP559; NAD83: 66.15591N, -62.44485W																							
9972-51.1	516	173	0.35	nd	nd	0.000042	151	0.07	155	0.100	4.4	5.459	1.7	0.3491	1.3	0.7734	0.1134	1.09	1930	22	1855	20	-4.7
9972-60.2	395	93	0.24	nd	nd	0.000064	27	0.11	105	0.066	6.0	4.860	1.5	0.3098	1.3	0.8904	0.1138	0.68	1740	20	1861	12	7.4
9972-37.1	501	243	0.50	nd	nd	0.000042	29	0.07	146	0.142	3.7	5.333	1.5	0.3384	1.4	0.9178	0.1143	0.60	1879	23	1869	11	-0.7
9972-14.1	397	139	0.36	nd	nd	0.000065	23	0.11	118	0.096	4.8	5.460	1.5	0.3449	1.3	0.8992	0.1148	0.65	1910	22	1877	12	-2.1
9972-40.2	494	165	0.35	nd	nd	0.000038	38	0.07	141	0.099	4.4	5.288	1.5	0.3320	1.4	0.9182	0.1155	0.60	1848	22	1888	11	2.4
9972-40.1	584	257	0.45	nd	nd	-0.000010	83	-0.02	168	0.129	3.5	5.360	1.4	0.3352	1.3	0.9281	0.1160	0.53	1864	21	1895	9	1.9
9972-29.1	261	71	0.28	nd	nd	0.000077	32	0.13	73	0.076	6.9	5.201	1.7	0.3249	1.5	0.8636	0.1161	0.85	1814	23	1897	15	5.1
9972-60.1	371	100	0.28	nd	nd	0.000000	100	0.00	108	0.075	5.9	5.435	1.6	0.3379	1.4	0.8288	0.1167	0.91	1876	22	1906	16	1.8
9972-14.2	279	122	0.45	nd	nd	-0.000139	43	-0.24	76	0.131	5.2	5.165	1.7	0.3175	1.4	0.8047	0.1180	1.01	1777	21	1926	18	8.8
9972-44.1	156	60	0.40	nd	nd	-0.000208	5	-0.36	46	0.114	7.3	5.639	1.8	0.3442	1.5	0.8375	0.1188	0.97	1907	24	1938	17	1.9
9972-67.1	857	191	0.23	nd	nd	0.000407	16	0.71	298	0.051	4.0	8.164	1.5	0.4055	1.3	0.8820	0.1460	0.69	2194	24	2300	12	5.4
9972-35.2	784	54	0.07	nd	nd	0.000062	28	0.11	264	0.017	7.9	8.191	1.4	0.3928	1.3	0.9507	0.1512	0.42	2136	24	2360	7	11.1
9972-56.1	1079	92	0.09	nd	nd	0.000015	26	0.03	390	0.027	5.0	8.803	1.3	0.4209	1.3	0.9681	0.1517	0.33	2264	24	2365	6	5.0
9972-28.1	842	79	0.10	nd	nd	0.000084	32	0.14	325	0.027	5.6	10.134	1.4	0.4492	1.3	0.9526	0.1636	0.41	2392	26	2494	7	4.9
9972-31.1	848	77	0.09	nd	nd	0.000032	23	0.06	354	0.017	7.4	11.118	1.3	0.4867	1.3	0.9604	0.1657	0.37	2556	27	2514	6	-2.0
9972-16.1	908	83	0.09	nd	nd	0.000034	42	0.06	371	0.027	4.9	10.953	1.3	0.4759	1.3	0.9699	0.1669	0.32	2509	27	2527	5	0.8
9972-1.1	798	63	0.08	nd	nd	0.000013	47	0.02	323	0.022	7.7	10.943	1.4	0.4707	1.4	0.9560	0.1686	0.42	2487	28	2544	7	2.7
9972-3.1	815	58	0.07	nd	nd	0.000058	35	0.10	339	0.019	7.6	11.479	1.4	0.4844	1.3	0.9505	0.1719	0.43	2547	28	2576	7	1.4
9972-56.2	695	57	0.08	nd	nd	0.000022	29	0.04	259	0.025	6.4	10.321	1.5	0.4330	1.4	0.9629	0.1729	0.39	2319	27	2586	7	12.3
9972-45.1	787	55	0.07	nd	nd	0.000011	97	0.02	334	0.020	6.4	12.119	1.3	0.4939	1.3	0.9704	0.1780	0.32	2587	28	2634	5	2.1
9972-61.1	756	66	0.09	nd	nd	0.000031	21	0.05	329	0.023	5.8	12.538	1.4	0.5057	1.3	0.9713	0.1798	0.33	2638	29	2651	5	0.6
9972-54.1	715	58	0.08	nd	nd	0.000010	136	0.02	301	0.026	5.9	12.195	1.4	0.4904	1.3	0.9622	0.1804	0.37	2573	28	2656	6	3.8
9972-5.2	832	85	0.11	nd	nd	0.000000	100	0.00	352	0.029	5.5	12.339	1.4	0.4918	1.3	0.9434	0.1820	0.46	2579	28	2671	8	4.2
9972-33.1	756	61	0.08	nd	nd	0.000015	33	0.03	366	0.019	6.4	14.210	1.3	0.5643	1.3	0.9738	0.1826	0.30	2885	30	2677	5	-9.6
9972-70.1	844	37	0.05	nd	nd	0.000018	32	0.03	371	0.013	8.0	12.967	1.3	0.5115	1.3	0.9694	0.1839	0.33	2663	28	2688	5	1.1
9972-5.3	970	104	0.11	nd	nd	0.000019	151	0.03	434	0.030	4.9	13.413	1.3	0.5212	1.3	0.9635	0.1866	0.36	2704	28	2713	6	0.4
9972-5.1	801	58	0.07	nd	nd	0.000018	57	0.03	361	0.021	6.2	13.520	1.3	0.5247	1.3	0.9688	0.1869	0.33	2719	29	2715	5	-0.2
9972-12.2	441	296	0.69	nd	nd	0.000101	69	0.18	200	0.213	2.7	14.405	1.5	0.5273	1.4	0.9125	0.1981	0.61	2730	30	2811	10	3.5
9972-26.1	678	315	0.48	nd	nd	0.000032	35	0.06	323	0.144	2.6	15.289	1.3	0.5547	1.3	0.9676	0.1999	0.34	2845	30	2825	6	-0.8
9972-52.1	743	513	0.71	nd	nd	0.000016	37	0.03	357	0.204	1.9	15.472	1.3	0.5587	1.3	0.9766	0.2008	0.28	2861	30	2833	5	-1.2
9972-20.1	322	10	0.03	nd	nd	0.000025	138	0.04	162	0.005	18.0	16.630	1.5	0.5842	1.4	0.9410	0.2064	0.50	2966	33	2878	8	-3.8
9972-35.1	99	2	0.02	nd	nd	0.000073	47	0.13	48	0.002	42.3	16.167	1.9	0.5628	1.7	0.8789	0.2084	0.91	2878	39	2893	15	0.6
9972-18.1	176	13	0.08	nd	nd	0.000066	29	0.11	84	0.021	11.7	16.396	1.6	0.5568	1.5	0.9233	0.2136	0.61	2853	34	2933	10	3.4
9972-50.1	238	119	0.52	nd	nd	0.000051	34	0.09	117	0.140	4.3	16.919	1.5	0.5736	1.4	0.9315	0.2139	0.55	2922	33	2936	9	0.6
9972-64.1	252	240	0.98	nd	nd	0.000084	22	0.15	128	0.264	2.9	17.400	1.5	0.5899	1.4	0.9412	0.2139	0.51	2989	34	2936	8	-2.3
9972-6.1	307	167	0.56	nd	nd	0.000048	40	0.08	155	0.146	3.6	17.404	2.5	0.5892	2.5	0.9848	0.2142	0.44	2986	60	2938	7	-2.0
9972-62.1	114	4	0.04	nd	nd	0.000142	23	0.25	54	0.006	41.6	16.371	1.7	0.5529	1.6	0.8998	0.2148	0.76	2837	36	2942	12	4.4
9972-12.1	308	171	0.57	nd	nd	0.000000	100	0.00	164	0.158	3.4	18.454	1.4	0.6194	1.4	0.9565	0.2161	0.42	3107	34	2952	7	-6.7
9972-48.1	91	55	0.62	nd	nd	0.000090	41	0.16	45	0.176	5.9	16.995	2.8	0.5681	2.6	0.9505	0.2170	0.86	2900	61	2958	14	2.5
9972-67.2	282	189	0.69	nd	nd	0.000108	27	0.19	136	0.182	4.6	16.963	1.6	0.5618	1.5	0.9199	0.2190	0.63	2874	34	2973	10	4.1
09SRB-M145A (GSC lab number z9983) IP559; NAD83: 66.04860N, -63.34248W																							
9983-93.1	213	69	0.34	nd	nd	0.000163	27	0.28	61	0.099	7.4	5.197	1.9	0.3351	1.5	0.7869	0.1125	1.15	1863	24	1840	21	-1.4
9983-25.1	541	212	0.40	nd	nd	0.000056	24	0.10	160	0.031	7.5	5.380	1.4	0.3449	1.3	0.9120	0.1132	0.59	1910	22	1851	11	-3.7
9983-103.2	295	138	0.48	nd	nd	0.000061	90	0.11	86	0.137	4.3	5.390	1.7	0.3416	1.4	0.8221	0.1144	0.94	1895	22	1871	17	-1.5
9983-76.2	451	109	0.25	nd	nd	0.000041	26	0.07	140	0.062	5.7	5.739	1.5	0.3623	1.3	0.9099	0.1149	0.60	1993	23	1878	11	-7.1
9983-103.1	257	118	0.48	nd	nd	0.000000	100	0.00	77	0.117	6.3	5.537	1.7	0.3492	1.4	0.8500	0.1150	0.88	1931	24	1880	16	-3.2
9983-76.1	464	88	0.20	nd	nd	0.000026	137	0.05	137	0.052	6.4	5.453	1.5	0.3436	1.3	0.8749	0.1151	0.75	1904	22	1881	13	-1.4
9983-93.2	401	155	0.40	nd	nd	0.000000	100	0.00	113	0.108	4.5	5.247	1.7	0.3284	1.6	0.9308	0.1159	0.61	1831	25	1893	11	3.8
9983-102.1	523	243	0.48	nd	nd	0.000026	93	0.04	164	0.125	3.8	6.000	1.5	0.3651	1.3	0.9061	0.1192	0.62	2006	23	1944	11	-3.7
9983-44.1	1191	151	0.13	nd	nd	0.000017	38	0.03	462	0.037	4.2	9.979	1.3	0.4514	1.3	0.9725	0.1604	0.31	2401	26	2459	5	2.8
9983-75.1	1273	246	0.20	nd	nd	0.000033	38	0.06	506	0.057	3.0	10.341	1.3	0.4627	1.3	0.9763	0.1621	0.29	2452	26	2478	5	1.3
9983-32.1	138	147	1.11	nd	nd	0.000536	22	0.93	55	0.322	3.7	11.154	2.1	0.4642	1.7	0.8341	0.1742	1.15	2458	36	2599	19	6.5
9983-62.1	155	191	1.27	nd	nd	0.000212	31	0.37	68	0.350	3.6	12.756	1.8	0.5101	1.5	0.8642	0.1814	0.89	2657	33	2665	15	0.4
9983-106.1	121	200	1.71	nd	nd	0.002085	17	3.61	52	0.410	3.6	12.608	3.2	0.5026	1.7	0.5315	0.1819	2.71	2625	37	2671	45	2.1

Table 1. Continued.

Spot name	U (ppm)	Th (ppm)	Th/U	Yb (ppm)	Hf (ppm)	$^{204}Pb/^{206}Pb$	% ±	$f(206)^{204}$ %	$^{206}Pb^*$ (ppm)	$^{208*}Pb/^{206*}Pb$	% ±	$^{207*}Pb/^{235}U$	% ±	$^{206*}Pb/^{238}U$	% ±	Corr Coeff	$^{207*}Pb/^{206*}Pb$	% ±	Apparent ages (Ma) $^{206}Pb/^{238}U$	$\pm ^{206}Pb/^{238}U$	$^{207}Pb/^{206}Pb$	$\pm ^{207}Pb/^{206}Pb$	Disc. (%)
09SRB-M145A (GSC lab number z9983) IP559; NAD83: 66.04860N, -63.34248W (continued)																							
9983-14.1	169	194	1.18	nd	nd	0.000115	27	0.20	75	0.315	3.5	13.284	1.7	0.5177	1.5	0.9025	0.1861	0.73	2689	34	2708	12	0.9
9983-39.1	117	158	1.39	nd	nd	0.000000	100	0.00	52	0.364	4.1	13.357	1.8	0.5190	1.6	0.8800	0.1867	0.87	2695	35	2713	14	0.8
9983-21.1	99	158	1.66	nd	nd	0.000134	31	0.23	45	0.455	4.0	13.644	1.9	0.5254	1.7	0.8617	0.1883	0.98	2722	37	2728	16	0.2
9983-17.1	79	106	1.38	nd	nd	0.000191	40	0.33	37	0.368	4.6	14.018	2.0	0.5395	1.7	0.8397	0.1885	1.10	2781	39	2729	18	-2.4
9983-56.1	117	172	1.52	nd	nd	0.000112	28	0.19	54	0.427	3.5	13.863	1.8	0.5328	1.6	0.8864	0.1887	0.82	2753	35	2731	14	-1.0
9983-82.1	103	142	1.42	nd	nd	0.000059	47	0.10	48	0.392	4.0	14.044	1.8	0.5392	1.6	0.8772	0.1889	0.88	2780	36	2733	15	-2.1
9983-19.1	96	116	1.25	nd	nd	0.000000	100	0.00	43	0.324	4.3	13.627	1.9	0.5229	1.6	0.8811	0.1890	0.88	2711	36	2733	15	1.0
9983-10.1	130	222	1.76	nd	nd	0.000000	100	0.00	61	0.483	3.3	14.466	2.0	0.5499	1.8	0.9154	0.1908	0.79	2825	41	2749	13	-3.4
9983-94.1	112	143	1.32	nd	nd	0.000081	137	0.14	49	0.365	4.3	13.582	2.2	0.5150	1.9	0.8588	0.1913	1.14	2678	42	2753	19	3.3
9983-64.1	121	185	1.59	nd	nd	0.000448	25	0.78	54	0.386	3.9	13.810	2.1	0.5228	1.7	0.8365	0.1916	1.14	2711	38	2756	19	2.0
9983-87.1	147	184	1.29	nd	nd	0.000000	100	0.00	68	0.357	3.6	14.367	1.7	0.5430	1.5	0.8982	0.1919	0.75	2796	35	2759	12	-1.7
9983-74.1	79	115	1.51	nd	nd	0.000104	41	0.18	35	0.425	4.3	13.848	2.3	0.5227	1.7	0.7531	0.1921	1.52	2711	38	2761	25	2.2
9983-69.1	1873	78	0.04	nd	nd	0.000026	37	0.05	784	0.012	5.1	13.048	1.3	0.4874	1.3	0.9869	0.1942	0.21	2559	27	2778	3	9.5
9983-40.1	1405	113	0.08	nd	nd	0.000251	13	0.44	572	0.008	5.3	12.996	1.5	0.4741	1.5	0.9768	0.1988	0.32	2502	30	2816	5	13.5
9983-50.1	1867	87	0.05	nd	nd	0.000224	12	0.39	807	0.011	4.5	14.210	1.3	0.5029	1.3	0.9780	0.2049	0.27	2626	27	2866	4	10.2
9983-28.2	1429	67	0.05	nd	nd	0.000007	92	0.01	627	0.020	5.2	15.278	1.3	0.5108	1.3	0.9808	0.2169	0.25	2660	28	2958	4	12.3
9983-18.1	1239	263	0.22	nd	nd	0.000009	26	0.02	615	0.054	3.0	21.475	1.3	0.5778	1.3	0.9843	0.2696	0.23	2940	31	3303	4	13.7
9983-61.1	861	241	0.29	nd	nd	0.000231	18	0.40	460	0.069	2.9	23.568	1.3	0.6221	1.3	0.9731	0.2747	0.31	3118	32	3333	5	8.1
9983-46.1	400	364	0.94	nd	nd	0.000000	100	0.00	259	0.247	2.2	36.649	1.6	0.7558	1.5	0.9796	0.3517	0.31	3629	43	3714	5	3.0
9983-28.1	135	123	0.94	nd	nd	0.000067	93	0.12	97	0.237	3.4	44.620	1.7	0.8402	1.5	0.9162	0.3852	0.67	3932	45	3852	10	-2.8
07SAB-03 (GSC lab number z9896) IP529; NAD83: 64.94533N,-63.68333W																							
9896-41.2	72	6	0.08	nd	nd	0.001258	30	2.18	18	0.012	17.0	4.372	5.4	0.2889	1.7	0.3136	0.1097	5.17	1636	25	1795	94	10.0
9896-19.1	64	10	0.15	nd	nd	0.000430	23	0.75	20	0.029	18.7	6.420	2.0	0.3561	1.5	0.7465	0.1307	1.30	1964	25	2108	23	7.9
9896-4.2	69	6	0.09	nd	nd	0.000359	26	0.62	21	0.023	7.3	6.484	1.9	0.3571	1.4	0.7731	0.1317	1.19	1968	25	2121	21	8.3
9896-57.1	76	8	0.11	nd	nd	0.000262	24	0.45	24	0.023	6.7	7.272	1.6	0.3669	1.3	0.8101	0.1437	0.96	2015	23	2273	16	13.2
9896-76.1	52	5	0.10	nd	nd	0.000733	33	1.27	16	0.037	17.1	7.163	3.5	0.3521	2.2	0.6429	0.1475	2.67	1945	38	2318	46	18.6
9896-38.1	78	12	0.16	nd	nd	0.000544	36	0.94	24	0.064	13.2	7.481	2.8	0.3660	1.7	0.5945	0.1482	2.24	2010	29	2326	38	15.8
9896-40.3	67	11	0.17	nd	nd	0.000316	45	0.55	24	0.044	6.2	9.023	2.5	0.4199	2.0	0.8287	0.1559	1.38	2260	39	2411	23	7.4
9896-84.2	134	137	1.06	nd	nd	0.000042	38	0.07	49	0.294	1.7	9.477	1.3	0.4249	1.2	0.9346	0.1618	0.46	2283	23	2474	8	9.2
9896-40.1	75	10	0.14	nd	nd	0.000028	56	0.05	28	0.045	5.2	9.845	1.8	0.4375	1.3	0.7256	0.1632	1.23	2339	26	2489	21	7.2
9896-74.2	76	14	0.19	nd	nd	0.000425	22	0.74	31	0.045	5.3	11.167	1.7	0.4766	1.4	0.8289	0.1699	0.95	2512	29	2557	16	2.1
9896-28.1	88	16	0.19	nd	nd	0.000203	29	0.35	34	0.071	3.8	10.997	1.5	0.4530	1.3	0.8577	0.1761	0.77	2408	26	2616	13	9.5
9896-74.3	54	10	0.19	nd	nd	0.002817	18	4.88	21	0.077	9.1	11.545	4.8	0.4584	2.8	0.5695	0.1827	3.97	2433	56	2677	66	11.0
9896-22.1	74	15	0.21	nd	nd	0.000153	24	0.26	34	0.052	4.8	14.073	1.6	0.5442	1.5	0.9306	0.1876	0.58	2801	34	2721	10	-3.6
9896-61.1	184	9	0.05	nd	nd	0.000046	33	0.08	83	0.012	6.0	13.704	1.2	0.5290	1.2	0.9588	0.1879	0.34	2737	26	2724	6	-0.6
9896-53.1	173	14	0.08	nd	nd	0.000127	33	0.22	78	0.018	4.7	13.782	1.2	0.5282	1.2	0.9392	0.1892	0.42	2734	26	2736	7	0.1
9896-40.2	604	27	0.05	nd	nd	0.000007	23	0.01	266	0.011	6.0	13.366	1.1	0.5119	1.1	0.9840	0.1894	0.19	2665	23	2737	3	3.2
9896-86.2	42	43	1.05	nd	nd	0.000238	35	0.41	19	0.272	2.7	13.970	1.7	0.5341	1.5	0.8702	0.1897	0.86	2759	34	2740	14	-0.9
9896-26.1	158	48	0.32	nd	nd	0.000023	255	0.04	71	0.086	2.4	13.785	1.3	0.5260	1.2	0.8981	0.1901	0.57	2725	26	2743	9	0.8
9896-65.1	248	40	0.16	nd	nd	0.000044	29	0.08	111	0.043	2.9	13.650	1.2	0.5206	1.2	0.9541	0.1902	0.36	2702	25	2744	6	1.9
9896-33.1	216	35	0.17	nd	nd	0.000031	61	0.05	98	0.045	3.3	13.939	4.5	0.5312	1.2	0.2569	0.1903	4.39	2747	26	2745	72	-0.1
9896-46.2	281	10	0.04	nd	nd	0.000010	62	0.02	125	0.010	5.4	13.690	1.1	0.5186	1.1	0.9729	0.1915	0.26	2693	24	2755	4	2.7
9896-84.1	349	20	0.06	nd	nd	0.000015	39	0.03	161	0.016	3.6	14.172	1.2	0.5356	1.2	0.9739	0.1919	0.27	2765	26	2758	4	-0.3

Notes (*see* Stern, 1997):
Spot name follows the convention x-y.z; where x = sample number, y = grain number, and z = spot number. Multiple analyses in an individual spot are labelled as x-y.z.z
Uncertainties reported at 1s and are calculated by using SQUID 2.23.08.10.21, rev. 21 Oct 2008
nd = not determined
$f206^{204}$ refers to mole percent of total ^{206}Pb that is due to common Pb, calculated using the ^{204}Pb-method; common Pb composition used is the surface blank (4/6: 0.05770; 7/6: 0.89500; 8/6: 2.13840)
* refers to radiogenic Pb (corrected for common Pb)
Discordance relative to origin = 100 * ((207/206 age -206/238 age)/($^{207}Pb/^{206}Pb$ age))
Calibration standard 6266; U = 910 ppm; Age = 559 Ma; $^{206}Pb/^{238}U = 0.09059$
Analytical details
IP529: 35 µm spot; analyses marked with * analysed using 9 µm spot; 6 scans; U-Pb calibration error 1% (included);
Measured age of secondary standard 1242 = 2675 ± 4 Ma (n = 12); no mass fractionation correction.
IP559: 16 µm spot; 5 scans; U-Pb calibration error 1.23% (included);
Measured age of secondary standard 1242 = 2677 ± 8 Ma (n = 16); no mass fractionation correction.

Table 1. Continued.

Spot name	U (ppm)	Th (ppm)	Th/U	Yb (ppm)	Hf (ppm)	$^{204}Pb/^{206}Pb$	% ±	$f(206)^{204}$ %	$^{206}Pb^*$ (ppm)	$^{208*}Pb/^{206*}Pb$	% ±	$^{207*}Pb/^{235}U$	% ±	$^{206*}Pb/^{238}U$	% ±	Corr Coeff	$^{207*}Pb/^{206*}Pb$	% ±	Apparent ages (Ma) $^{206}Pb/^{238}U$	$\pm^{206}Pb/^{238}U$	$^{207}Pb/^{206}Pb$	$\pm^{207}Pb/^{206}Pb$	Disc. (%)
07SAB-03 (GSC lab number z9896) IP529; NAD83: 64.94533N,-63.68333W (continued)																							
9896-77.1	102	4	0.04	nd	nd	0.000067	41	0.12	44	0.012	11.9	13.386	1.4	0.5058	1.3	0.8869	0.1919	0.65	2639	27	2759	11	5.3
9896-86.1	350	24	0.07	nd	nd	0.000044	23	0.08	162	0.016	4.1	14.261	1.3	0.5381	1.3	0.9773	0.1922	0.27	2776	28	2761	4	-0.6
9896-1.1	305	37	0.13	nd	nd	0.000003	87	0.01	145	0.034	2.6	14.727	1.1	0.5543	1.1	0.9808	0.1927	0.22	2843	25	2765	4	-3.5
9896-82.1	286	29	0.11	nd	nd	0.000020	25	0.03	129	0.028	3.3	13.979	1.1	0.5260	1.1	0.9733	0.1927	0.26	2725	24	2766	4	1.8
9896-8.1	251	33	0.14	nd	nd	0.000038	49	0.07	115	0.035	2.7	14.152	1.1	0.5325	1.1	0.9576	0.1928	0.33	2752	24	2766	5	0.6
9896-46.1	317	16	0.05	nd	nd	0.000013	53	0.02	143	0.013	4.2	13.912	1.1	0.5233	1.1	0.9658	0.1928	0.29	2713	24	2766	5	2.3
9896-74.1	150	30	0.21	nd	nd	0.000076	29	0.13	68	0.053	3.3	14.102	1.4	0.5296	1.3	0.9095	0.1931	0.57	2740	28	2769	9	1.3
9896-13.1	117	63	0.56	nd	nd	0.000047	66	0.08	54	0.152	2.1	14.277	1.3	0.5358	1.2	0.9190	0.1933	0.51	2766	27	2770	8	0.2
9896-28.2	330	16	0.05	nd	nd	0.000024	53	0.04	147	0.013	4.7	13.770	1.1	0.5167	1.1	0.9716	0.1933	0.27	2685	24	2770	4	3.8
9896-21.1	127	60	0.49	nd	nd	0.000072	14	0.13	59	0.127	2.2	14.499	1.3	0.5436	1.2	0.9317	0.1934	0.46	2799	27	2772	8	-1.2
9896-32.1	455	30	0.07	nd	nd	0.000012	28	0.02	206	0.019	3.2	14.033	1.3	0.5261	1.3	0.9878	0.1935	0.20	2725	29	2772	3	2.1
9896-54.1	193	25	0.13	nd	nd	0.000013	70	0.02	88	0.034	3.6	14.142	1.2	0.5299	1.1	0.9644	0.1936	0.31	2741	26	2773	5	1.4
9896-10.1	184	57	0.32	nd	nd	0.000070	25	0.12	87	0.087	2.1	14.638	1.4	0.5480	1.3	0.9584	0.1937	0.39	2817	30	2774	6	-1.9
9896-41.1	63	62	1.02	nd	nd	0.000204	32	0.35	29	0.270	2.2	14.237	1.5	0.5329	1.4	0.8974	0.1938	0.67	2754	31	2774	11	0.9
9896-48.1	74	85	1.18	nd	nd	0.000153	35	0.27	34	0.312	1.9	14.362	2.5	0.5374	2.4	0.9695	0.1938	0.60	2772	54	2775	10	0.1
9896-50.1	68	15	0.22	nd	nd	0.000380	75	0.66	27	0.091	10.5	12.544	2.7	0.4684	1.7	0.6266	0.1942	2.12	2476	35	2778	35	13.1
9896-23.1	38	29	0.79	nd	nd	0.000057	27	0.10	16	0.212	3.2	13.118	2.0	0.4892	1.8	0.9058	0.1945	0.86	2567	39	2780	14	9.3
9896-4.1	169	177	1.08	nd	nd	-0.000008	99	-0.01	77	0.288	1.3	14.234	1.2	0.5291	1.1	0.9622	0.1951	0.33	2738	26	2786	5	2.1
9896-7.1	73	87	1.23	nd	nd	0.000011	346	0.02	35	0.334	1.7	14.883	1.4	0.5531	1.3	0.8999	0.1951	0.61	2838	29	2786	10	-2.3
9896-34.1	35	53	1.54	nd	nd	-0.000073	59	-0.13	16	0.428	2.4	14.244	1.8	0.5259	1.6	0.9079	0.1964	0.74	2724	35	2797	12	3.2

Notes (*see* Stern, 1997):
Spot name follows the convention x-y.z; where x = sample number, y = grain number, and z = spot number. Multiple analyses in an individual spot are labelled as x-y.z.z
Uncertainties reported at 1s and are calculated by using SQUID 2.23.08.10.21, rev. 21 Oct 2008
nd = not determined
$f206^{204}$ refers to mole percent of total ^{206}Pb that is due to common Pb, calculated using the ^{204}Pb-method; common Pb composition used is the surface blank (4/6: 0.05770; 7/6: 0.89500; 8/6: 2.13840)
* refers to radiogenic Pb (corrected for common Pb)
Discordance relative to origin = 100 * ((207/206 age -206/238 age)/($^{207}Pb/^{206}Pb$ age))
Calibration standard 6266; U = 910 ppm; Age = 559 Ma; $^{206}Pb/^{238}U$ = 0.09059
Analytical details
IP529: 35 µm spot; analyses marked with * analysed using 9 µm spot; 6 scans; U-Pb calibration error 1% (included);
Measured age of secondary standard 1242 = 2675 ± 4 Ma (n = 12); no mass fractionation correction.

yielded an age within the older population. This nonreproducibility, both within and between grains, suggests that incomplete lead loss is the likely cause of the younger results.

09SRB-M106A (z10464)

The Canyon Wash locality is a spectacular glacial meltwater–washed exposure of plutonic rocks cut by a network of deformed sills and undeformed dykes (Fig. 3a) on central Cumberland Peninsula (Fig. 1). A sample of fine-grained, equigranular, biotite granodiorite was collected from compositionally-banded and -sheeted straight mylonite gneiss (Fig. 3b). Abundant, large, stubby prismatic zircon was recovered. Most grains are clear, colourless and faintly zoned in back-scattered electron images. Rare grains exhibit pale brown tips or overgrowths, which in back-scattered electron images show an enhanced response consistent with higher U content. Thirty-seven analyses were carried out on 28 separate zircon grains (Fig. 3c). Analyses of the clear, colourless zoned zircon yields dates ranging from 2954 Ma to 2891 Ma. These dates are clustered toward the older values, a pattern consistent with incomplete lead loss. The weighted mean $^{207}Pb/^{206}Pb$ age of the oldest 15 analyses, which includes replicates on single grains, is 2938 ± 4 Ma and is considered the best estimate for the age of crystallization of the granodiorite. Analyses of the high U rims range from 2738 Ma to 2430 Ma, and do not form a distinct grouping. This variability in the data does not allow timing constraints on the thermal and/or fluid event(s) responsible for these overgrowths, except to constrain the latest event to sometime after 2.43 Ga.

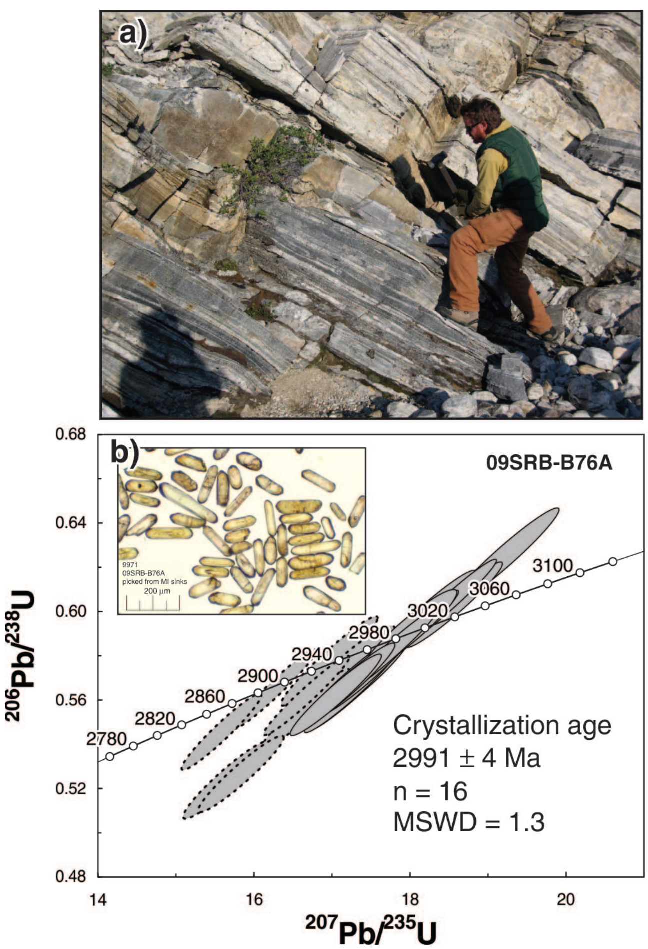

Figure 2. a) Sample 09SRB-B076A taken from the brown-weathering layer at roughly knee-level of the geologist (height of geologist approximately 173 cm). 2012-054. **b)** Concordia diagram of SHRIMP U-Pb results. Analyses excluded from the calculation of the weighted mean are shown by dashed ellipses.

09SRB-M100A (z9979)

Throughout the southern part of the map sheet, the relationship between the dominant tonalite-granodiorite and the thin panels of metasedimentary rock is highly tectonized. Primary contacts such as unconformities or intrusive contacts are rare. An outcrop north of Kumlien Fiord (Fig. 1) is one such example where there is a demonstrable intrusive relationship by virtue of exposed contacts between monzogranite and a panel of garnet-biotite semipelite and the presence of garnet in monzogranite at the contact (Fig. 4a). The recovered zircon grains are characterized by faint concentric zoning in back-scattered electron images. Rare grains have thin, high U (bright in back-scattered electron images), unzoned rims. Twenty-six analyses were carried out on twenty-three separate zircon grains (Fig. 4b). The dominant zircon population is centred at ca. 2780 Ma, with several analyses both older and younger. The weighted mean $^{207}Pb/^{206}Pb$ age of 13 analyses is 2782 ± 4 Ma and is interpreted as the crystallization age. Older single phase zircon crystals and rare cores dated at 2.80 Ga, 2.87 Ga, and 2.89 Ga are interpreted as inherited. Analysis of high U rims yield concordant, but not reproducible results between 2.7 Ga and 2.46 Ga. The timing of growth and geological significance of these rims is not clear; however, they imply a recrystallization event sometime after 2.46 Ga. Intermediate ages between 2.76 Ga to 2.7 Ga, not included in the calculation of the weighted mean crystallization age, are interpreted to represent lead loss from the igneous population. This monzogranite provides evidence for an Archean sedimentary package older than 2.78 Ga.

10SRB-M197A (z10462)

A sample of medium-grained, equigranular, moderately foliated, light grey biotite monzogranite (Fig. 5a) was collected from a discrete, aeromagnetically defined pluton south of Kumlien Fiord (Fig. 1; *see also* Sanborn-Barrie (2011a, Fig. 2)). Abundant pale brown, prismatic zircon was recovered. Back-scattered electron imaging reveals concentric zoning and rare overgrowths. In some instances, overgrowths are perfectly concordant with the zoning in the ‘core’ and may simply reflect changing magma compositions. SHRIMP analysis of thirty-one zircon grains yield ages ranging from 2881 Ma to 2640 Ma (Fig. 5b). Two primary groupings appear in these data, one centred at ca. 2.78 Ga and a second at 2.76 Ga (Fig. 5c). There is no clear morphological or chemical distinction between the two groups; however, as the oldest rim yields an age of 2768 Ma, the authors consider that it defines the upper age limit of the younger group. The weighted mean $^{207}Pb/^{206}Pb$ age of thirteen analyses between 2768 Ma and 2752 Ma is 2759 ± 3 Ma and is interpreted as the crystallization age of the monzogranite. The 2.88–2.77 Ga zircon grains are interpreted as inherited. The dominant 2.78 Ga inherited age is similar to the interpreted crystallization age of 09SRB-M100A, the host into which this discrete pluton was emplaced. Xenoliths of tonalite gneiss are observed at the margin of the pluton. Younger, nonreproducible dates between 2743 Ma and 2640 Ma, including the analysis of a number of rims, are interpreted to represent Pb loss from either of these older populations.

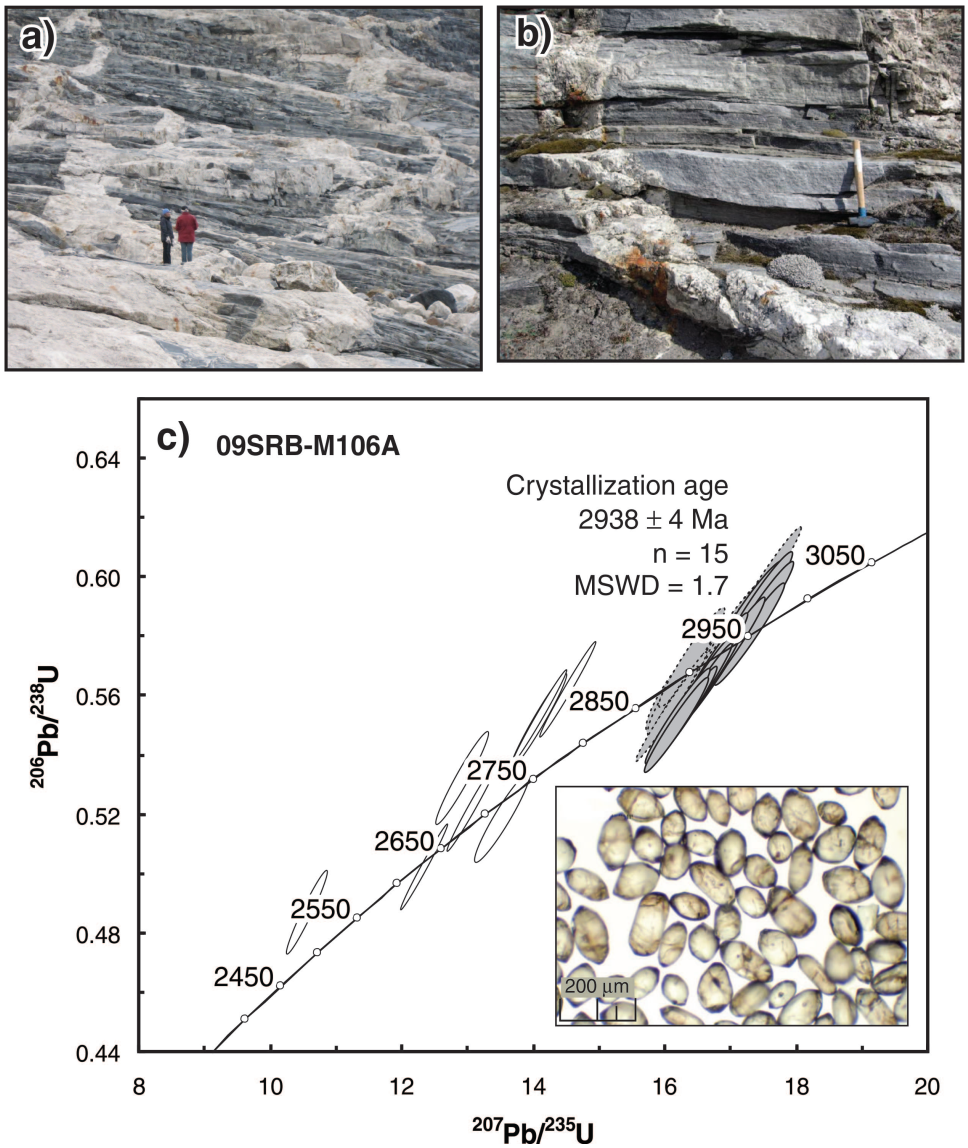

Figure 3. a) Overview photo of Canyon Wash locality where the Archean gneiss complex is cut by a network of undeformed pegmatite dykes. Height of people approximately 173 cm. 2012-045. **b)** Sample 09SRB-M106A was collected from the relatively homogeneous layer against which the hammer (45 cm) is resting. 2012-048. **c)** Concordia diagram of SHRIMP U-Pb results. Analyses from low U zircon cores are shown in grey, those excluded from the calculation of the weighted mean are outlined by dashed ellipses. White ellipses represent analyses from zircon overgrowths.

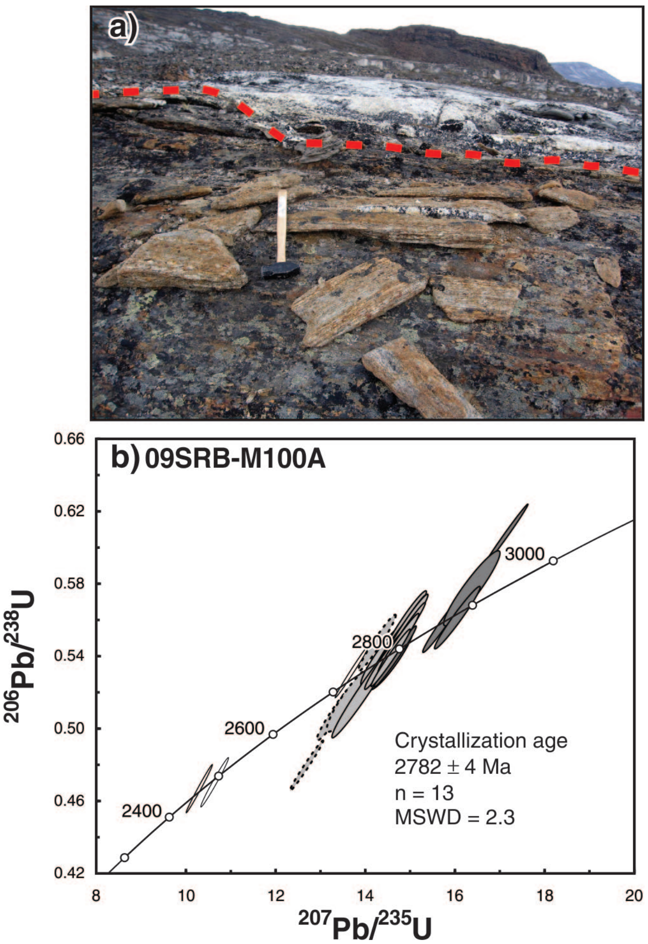

Figure 4. a) Sampling locality of 09SRB-M100A with monzogranite in the middle ground intruding into psammite (foreground). Dashed red line indicates approximate intrusive contact. Hammer (45 cm) for scale. 2012-057. **b)** Concordia diagram of SHRIMP U-Pb results. Dark grey ellipses represent inherited zircon, light grey ellipses are interpreted as igneous, with the analyses excluded from the calculation of the weighted mean outlined by dashed ellipses. White ellipses illustrate the results from rims.

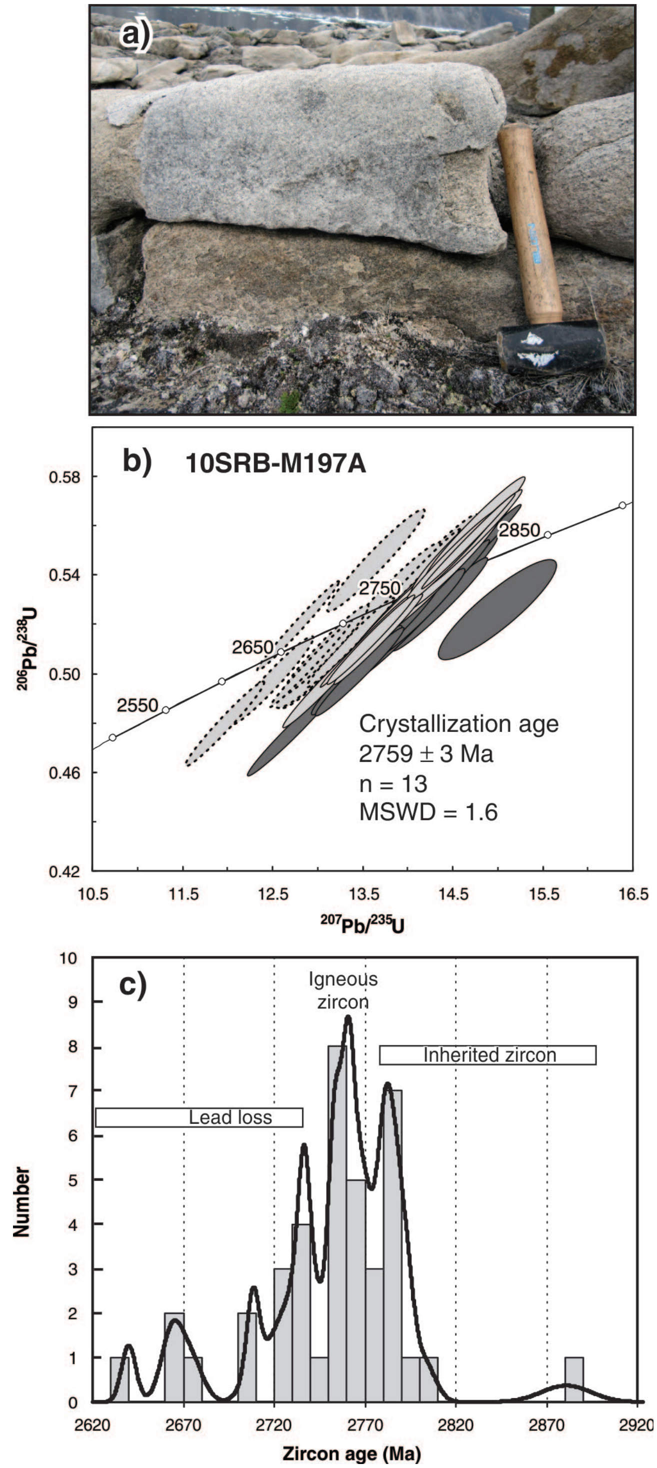

Figure 5. a) Photograph of monzogranite 09SRB-M197A. Hammer (30 cm) for scale. 2012-051. **b)** Concordia diagram of SHRIMP U-Pb results. Dark grey ellipses represent inherited zircon, light grey ellipses are interpreted as igneous, with the analyses excluded from the calculation of the weighted mean outlined by dashed ellipses. **c)** Probability density diagram illustrating distribution of zircon ages.

09SRB-D042A (z9974)

The Exaluin stock is a composite pluton exposed on the southeast coast of Cumberland Peninsula (Fig. 1), characterized by a magnetic high (*see* Sanborn-Barrie (2011c, Fig. 2)). It comprises brown-weathering, orthopyroxene- and magnetite-bearing, K-feldspar megacrystic monzogranite (Fig. 6a), typically exposed as inclusions within a pink-weathering, equigranular granite (Fig. 7a). Both phases contain a single, variably oriented, moderately developed foliation. Sample 09SRB-D042A, from the brown-weathering, charnockitic phase, yielded prismatic and well faceted to equant zircon. Careful examination of zoning patterns in back-scattered electron images allows discrimination of two zircon groups: a predominant group of faint concentric- to straight-zoned zircon, both as single phase grains and cores, and a second group of unzoned rims or tips. Forty-two analyses, carried out on 34 separate grains, yielded ages ranging from 2818 Ma to 2689 Ma. The weighted mean $^{207}Pb/^{206}Pb$ age of the 16 oldest zoned grains and cores is 2772 ± 6 Ma and is interpreted as the crystallization age of the charnockite.

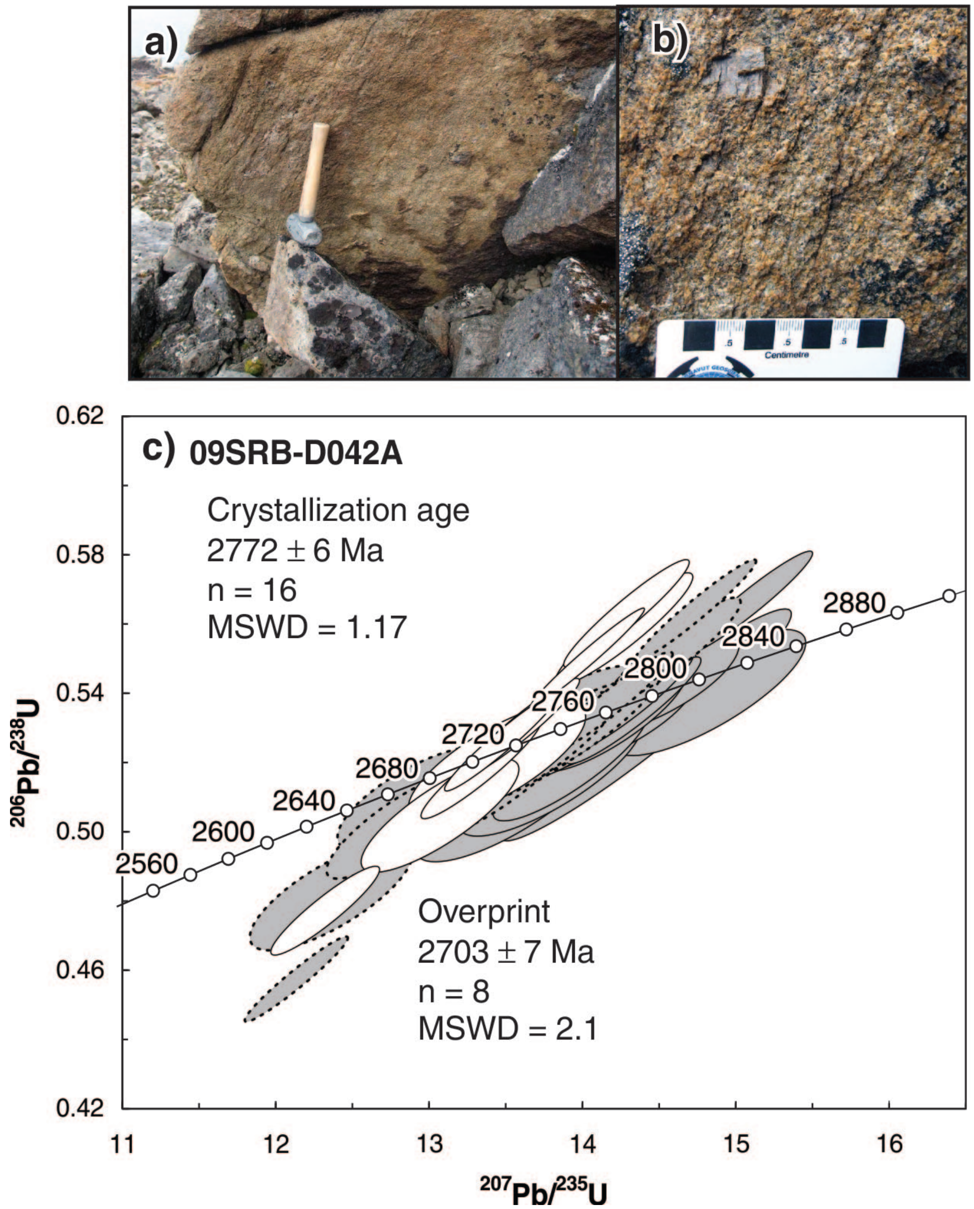

Figure 6. a) Brown-weathering, K-feldspar megacrystic granite 09SRB-D042A. Hammer (30 cm) for scale. 2012-050. **b)** Detail of megacrystic texture. 2012-053. **c)** Concordia diagram of SHRIMP U-Pb results. Light grey ellipses are interpreted as igneous, those excluded from the calculation of the weighted mean are outlined by dashed ellipses. White ellipses represent analyses from unzoned rims used to calculate the weighted mean age of the overprint.

Eight analyses of unzoned overgrowths yield a weighted mean $^{207}Pb/^{206}Pb$ age of 2703 ± 7 Ma. This overprint may be related to the emplacement of the equigranular granite that hosts the charnockitic enclaves. Some analyses of zoned zircon drift toward these younger ages, but do not form a distinct group. These are interpreted to have lost variable amounts of Pb during the overprinting event.

09SRB-D040B (z9973)

Pink-weathering equigranular monzogranite forms the dominant, younger phase of the Exaluin stock (Fig. 7a). A representative sample yielded abundant pale brown, prismatic zircon grains along with fewer clear, colourless crystals, occasionally preserved as cores. Archean ages were derived from all 45 analyses of 35 different zircon grains (Fig. 7b). A distinct group composed of 12 analyses of high U, unzoned zircon yield a weighted mean $^{207}Pb/^{206}Pb$ age of 2700 ± 4 Ma, which is interpreted as the crystallization age of this equigranular monzogranite. Other chemically and morphologically similar grains skew to slightly younger ages (Fig. 7b, inset), attributed to Pb loss. Colourless, low U cores and single-phase zoned zircon yield an indistinct swath of ages broadly 2.78–2.72 Ga, with rare Mesoarchean zircon. These are interpreted as an inherited component that is consistent with the crystallization age of the charnockitic phase into which this monzogranite was emplaced.

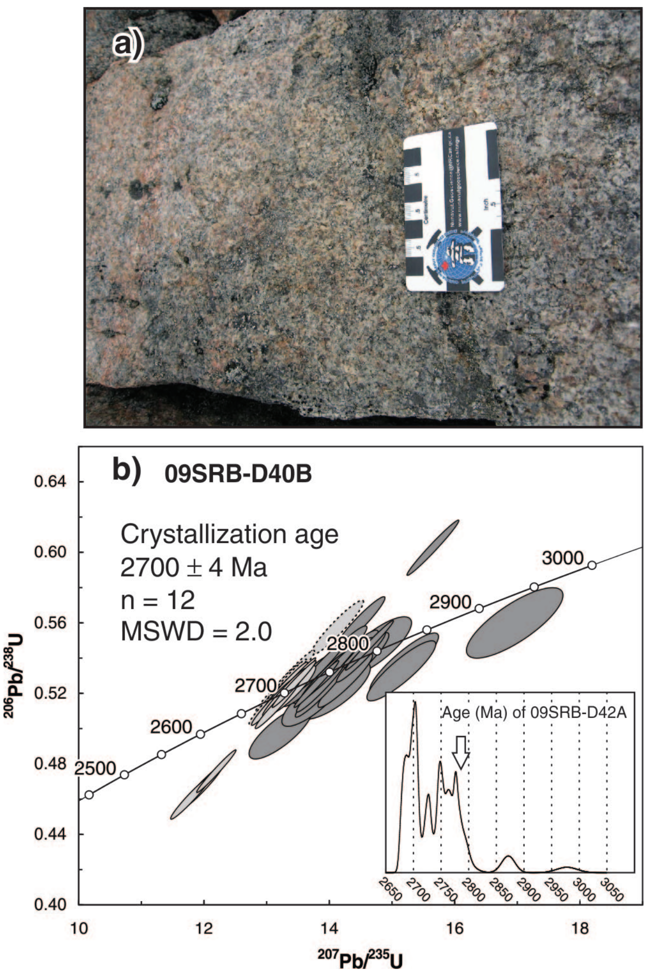

Figure 7. a) Photograph of the equigranular monzogranite 09SRB-D040B. 2012-055. **b)** Concordia diagram of SHRIMP U-Pb results. Light grey ellipses represent analyses of high-uranium, unzoned zircon that are used to calculate the weighted mean crystallization age. Dashed ellipses represent analyses that are excluded from the calculation. Dark grey ellipses are interpreted as inherited results. Inset probability density diagram illustrates the dominant 2.7 Ga population with skewness to older (inherited) ages.

07SAB-002 (z10151)

A sample of biotite-hornblende-magnetite±orthopyroxene monzogranite was collected from the eastern shore of Pangnirtung Fiord on Aulatsivik Point (Fig. 1), a locality thought to expose the eastern margin of the 1.865–1.845 Ga Cumberland Batholith (Whalen et al., 2010). This brown-weathering rock is strongly foliated (Fig. 8a, b) and inferred to have reached granulite facies. Zircon recovered from this monzogranite is colourless to medium brown, and is characterized by numerous inclusions and fractures (Fig. 8c inset). In plane light some grains appear to have light brown overgrowths. In back-scattered electron images, these grains are composed of single-phase, oscillatory zoned zircon or zoned zircon cores with unzoned back-scattered electron bright, high-uranium rims. There is extensive age and compositional (Th/U) overlap between the low-uranium cores and the high-uranium rims, with the cores only slightly older. The weighted mean $^{207}Pb/^{206}Pb$ age of the oldest 15 analyses (excluding the oldest analysis interpreted as inherited) yields an age of 1894 ± 5 Ma. An additional seven analyses of the same morphology yields ages as young at 1847 Ma. Nine analyses of high-uranium rims give ages that range from 1886–1844 Ma, although most are younger than 1860 Ma. The weighted mean $^{207}Pb/^{206}Pb$ age of the six youngest rim analyses is 1852 ± 8 Ma. On the basis of core-rim relationships and differences in zoning, the authors interpret these results to indicate crystallization of the monzogranite at 1894 ± 5 Ma, followed by 1852 ± 8 Ma high-grade metamorphism. Anomalously young ages from cores and anomalously old ages from rims are likely the result of lead loss and/or incomplete recrystallization during metamorphism, respectively.

09SRB-M109A (z10150)

Medium-grained, weakly foliated, biotite-hornblende-garnet monzogranite was collected from a dramatic flat-topped tower (Fig. 9a) located southeast of the boundary of Auyuittuq National Park (Fig. 1). This sample, with its diagnostic clusters of deep-red garnet (Fig. 9a inset), is representative of the noncharnockitic component of this extensive plutonic belt. Large, fractured, prismatic zircon has irregular outer surfaces suggesting partial resorption. Back-scattered electron images record faint, broad, concentric zoning, with no obvious core-rim relationships.

Thirty-two analyses of twenty-five zircon grains reveal a fairly simple zircon population. Twenty-four of the analyses yield a weighted mean $^{207}Pb/^{206}Pb$ age of 1889 ± 3 Ma, which is interpreted to represent the crystallization age of the monzogranite. Four analyses from three grains yield older ages between 1934 Ma and 2226 Ma, interpreted as inherited. Four zircon grains yield slightly younger ages, between 1868 Ma and 1853 Ma. As these results do not correspond to distinct zircon zones and are not replicated by repeat analyses the authors interpret these younger ages as the result of small amounts of lead loss.

09SRB-D010C (z9972)

At this locality, the contact zone between tonalite gneiss and metasedimentary rocks is demarcated by two distinctive chert horizons (Fig. 10a) and by interlayering between similar looking tonalite and psammite (Fig. 10b). As such, it was uncertain whether an unconformable, intrusive or

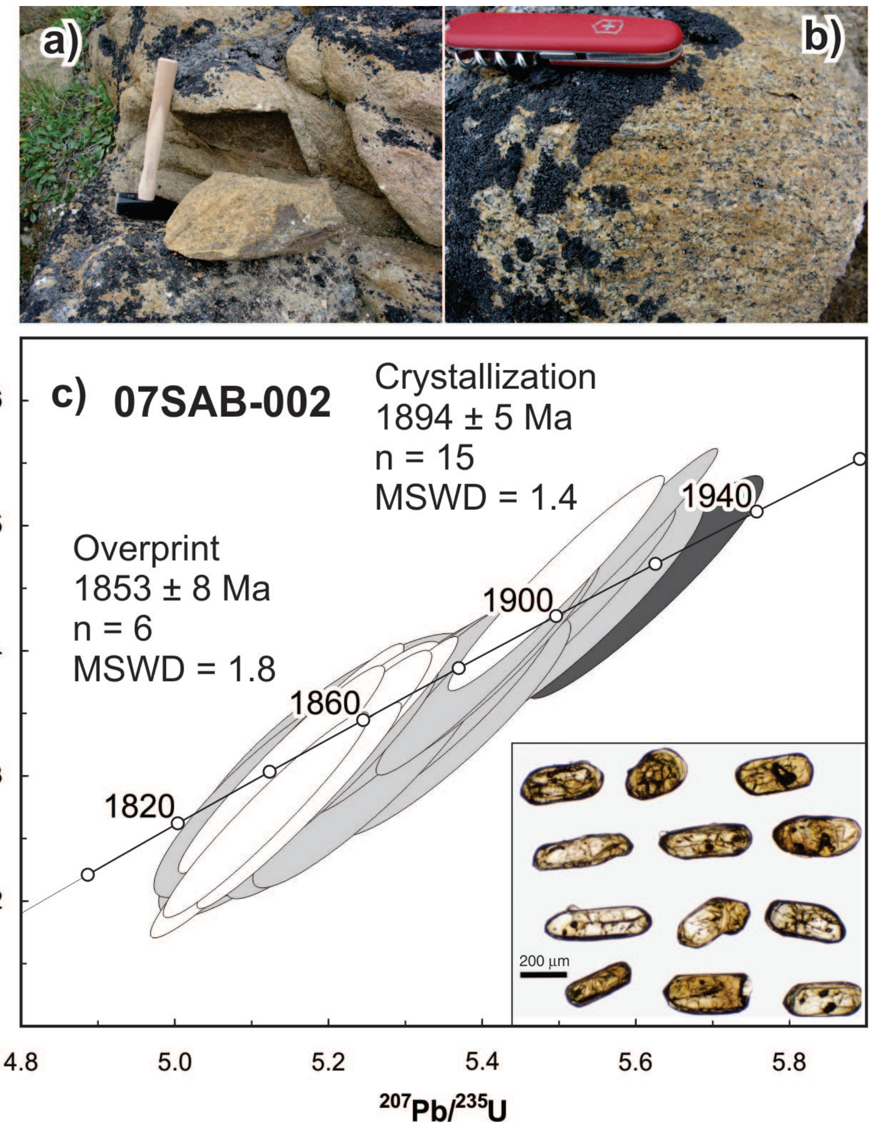

Figure 8. a) Brown-weathering, monzogranite 07SAB-002. Hammer (45 cm) for scale. 2012-043. **b)** Detail of foliation and weathering texture. Penknife (9 cm) for scale. 2012-041. **c)** Concordia diagram of SHRIMP U-Pb results. Single dark grey ellipses is interpreted as an inherited zircon. Light grey ellipses are from zoned zircon grains interpreted as igneous. White ellipses represent analyses from unzoned rims. Inset: plane-light image of zircon illustrating the internal structure of the grains. The two grains to the left in the upper row have light brown overgrowths.

tectonic contact relationship was preserved. Given that this was one of the few potential basement-cover contact zones in the map area, further insight was sought through dating of a homogeneous layer of medium-grained, equigranular, well foliated biotite tonalite. This layer is within a heterogeneous tonalite gneiss within 2 m of the first exposure of supracrustal-dominated outcrops.

The majority of the zircon grains are characterized by an elongate, prismatic morphology and fine-scale zoning in back-scattered electron images. These grains yield a wide range of variably discordant $^{207}Pb/^{206}Pb$ ages, from 2.97 Ga to 2.3 Ga (Fig. 10c). A subordinate population of large stubby zircon, typically characterized by faint, broad zoning in back-scattered electron images, yields a weighted mean $^{207}Pb/^{206}Pb$ age of 1882 ± 13 Ma, which may represent the crystallization age (Fig. 10c and inset). A Paleoproterozoic crystallization age is consistent with later injection into the gneiss complex. In this scenario, the 2.97 Ga to 2.3 Ga zircon grains are inherited from the interleaved tonalite gneiss complex and/or metasedimentary rocks. Given the complexity of the outcrop and the diversity of ages, it is permissible that the data record exclusively detrital zircon from the adjacent psammite. In this instance, 1882 Ma is most conservatively considered a maximum age for the tonalite.

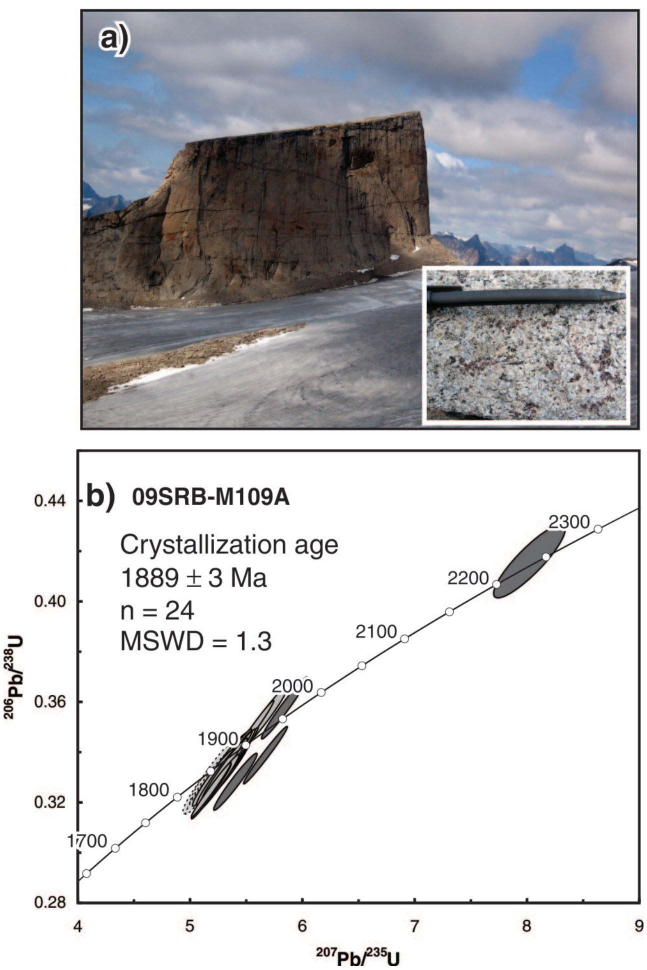

Figure 9. a) Flat-topped upland from which sample 09SRB-M109A was collected. Cliff is approximately 1000 m high. Inset shows detail of white-weathering surface and small clusters of dark red garnet. Field of view 12 cm. 2012-047. **b)** Concordia diagram of SHRIMP U-Pb results. Dark grey ellipses represent inherited zircon, light grey ellipses are interpreted as igneous, with the analyses excluded from the calculation of the weighted mean outlined by dashed ellipses.

09SRB-M145A (z9983)

A sample of mylonitic aplite was collected within a high-strain zone that straddles the contact between the Archean plutonic complex and the Hoare Bay Group about 75 km along strike from sample 09SRB-D010C (Fig. 1). The sample was collected from a region where exposures of hinges of gently plunging, tightly folded mylonitic aplite are proximal to foliated, but less deformed metavolcanic rocks (Fig. 11a, b). Zircon recovered from the aplite is highly variable in size, colour, and morphology. It varies from small (50 µm), clear, colourless to pale orange prisms to moderately sized (100 µm) turbid orange-brown prisms to relatively large (150–200 µm) clear, fractured prisms. The smaller clear and turbid grains yield $^{207}Pb/^{206}Pb$ ages ranging from 3852 Ma to 2459 Ma (Fig. 11c). Amongst these analyses, a cluster of ages at 2.74 Ga is characterized by distinctly high Th/U (Table 1). Four of the large, fractured prisms yielded a mean $^{207}Pb/^{206}Pb$ age of 1873 ± 16 Ma (n = 7 including replicate analyses, Fig. 11c inset). These Paleoproterozoic zircon grains are interpreted to represent the crystallization age of the aplite, rather than in situ metamorphism, based on their relatively high Th/U (ca. 0.3), oscillatory zoning in back-scattered electron images and their relatively large size. The older grains, including one large fractured prism with an age of 1944 Ma, are interpreted as inherited. A ca. 1.87 Ga crystallization age is consistent with the field interpretation that this aplite was emplaced syntectonically.

07SAB-003A (z9896)

The southernmost tip of Cumberland Peninsula at Cape Mercy (Fig. 1) exposes a complex chaotic gneiss (Fig. 12a), the age and ancestry of which was investigated for comparison to gneissic rocks elsewhere. A grey-weathering, homogeneous foliated monzogranite layer (Fig. 12b) was selected for geochronology. Back-scattered electron imaging of the zircon grains indicate a dominant population of oscillatory-zoned zircon. Unzoned rims are observed on many of the grains. The majority of analyses of zoned zircon yield $^{207}Pb/^{206}Pb$ ages that cluster around ca. 2.77 Ga, whereas unzoned zircon rims yield younger discordant results as young as 1.8 Ga (Fig. 12c). Although an initial preliminary interpretation of these results pointed toward crystallization at ca. 2.77 Ga, subsequent Sm-Nd isotopic tracer analyses indicate a depleted mantle model age of 2.42 Ga and an εNd value of 9.1 (at t = 2.77 Ga, J.B. Whalen, npub. data (2012)). This εNd value is higher than predicted from depleted mantle at ca. 2.77 Ga, revealing that the zircon population is more likely to be inherited. The combined zircon U-Pb and Nd isotopic results suggest mixing of a 2.77 Ga source with a younger juvenile magmatic component; however, given the available zircon data, the age of crystallization remains obscure. Nonetheless, this outcome does highlight the importance in utilization of several isotopic systems to ensure extraction of geologically meaningful information.

DISCUSSION AND CONCLUSIONS

Variably foliated to gneissic plutonic rocks are now recognized to dominate southern Cumberland Peninsula and these comprise a Mesoarchean component, including tonalite (09SRB-B76A), which yielded an age of 2991 ± 4 Ma and granodiorite (09SRB-M106A), with a crystallization age of 2938 ± 4 Ma. A third sample is represented by monzogranite north of Kumlien Fiord (09SRB-M100A) that yields a Neoarchean age of 2782 ± 4 Ma. Its clear intrusive relationship with a panel of metasedimentary rocks, establishes the presence of Archean supracrustal rocks. Similar

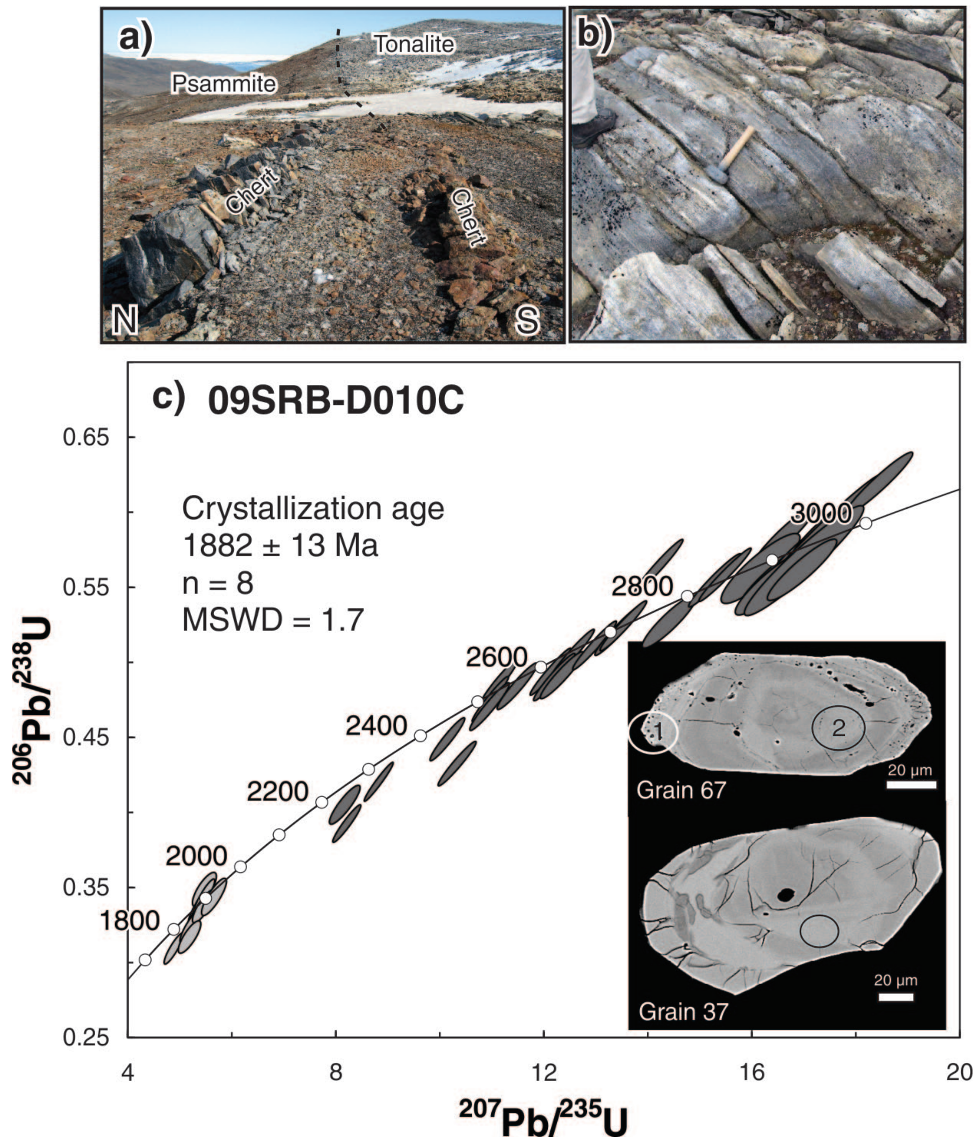

Figure 10. a) Field relationships for sample 09SRB-D010C. *See* text for discussion. Hammer on northern chert outcrop is 30 cm long. 2012-049. **b)** Detail of geochronology sampling location showing centimetre-scale banding. Hammer (30 cm) for scale. 2012-044 **c)** Concordia diagram of SHRIMP U-Pb results. Dark grey ellipses represent inherited zircon (i.e. grain 67). Light grey ellipses are analyses from large zoned grains (i.e. grain 37) that are interpreted as igneous. Ellipses correspond to analysis sites 9972-67.1, 9972-67.2, and 9972-37.1 in Table 1.

relationships between tonalite and thin supracrustal strands are observed across the southern half of the peninsula suggesting that supracrustal rocks of Archean age may be widespread (Sanborn-Barrie et al., 2011b). That this plutonic complex is structurally below the Hoare Bay Group establishes it as Meso- to Neoarchean structural basement complex.

Discrete Neoarchean plutons, reflected in the aeromagnetic data, are documented in both the eastern and southwestern parts of the peninsula. In the east, the Exaluin stock is a composite body with 2772 ± 6 Ma charnockite (09SRB-D042A) into which the more dominant noncharnockitic phase (09SRB-D040B) was emplaced at 2700 ± 4 Ma. The Sm-Nd isotope systematics also support a Neoarchean age for the Exaluin stock. There is no evidence of a Paleoproterozoic origin or overprint in either of the samples. In the southwest, the Kumlien stock (10SRB-M197A) is interpreted to have crystallized at 2759 ± 3 Ma. Further geochemical studies will evaluate if there is any petrogenetic link between these suites as well as the similarly aged monzogranite at Kumlien Fiord (09SRB-M100A).

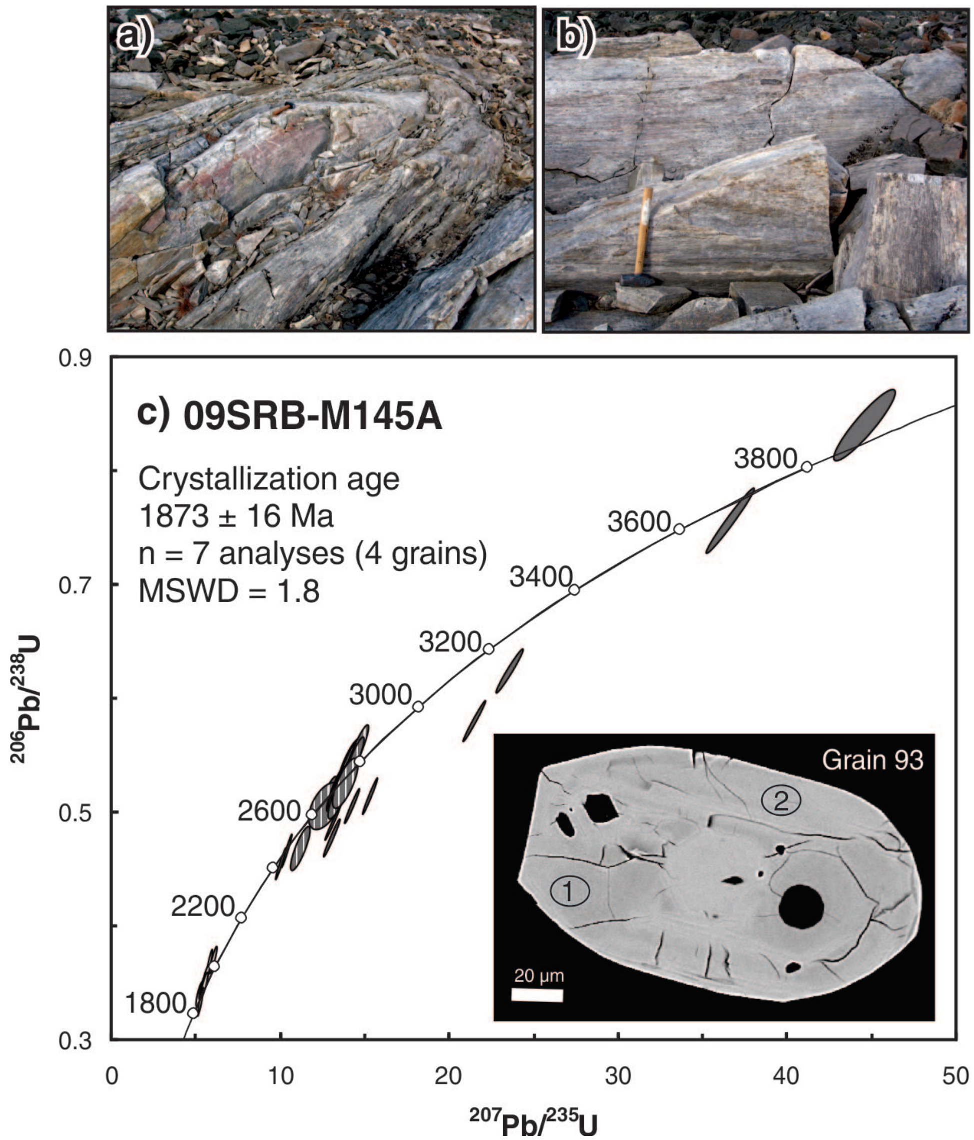

Figure 11. a) Exposed hinge of syntectonic aplite 09SRB-M145A. Enveloping mafic volcanic rocks are seen as rubble in the top left corner of the photograph. Hammer (30 cm) for scale. 2012-042. **b)** Detail of geochronology sample and mylonitic texture. Hammer (45 cm) for scale. 2012-056. **c)** Concordia diagram of SHRIMP U-Pb results. Dark grey ellipses represent inherited zircon, as do striped ellipses from a geochemically distinct 2.74 Ga population. Light grey ellipses are analyses from large zoned grains, interpreted as igneous (i.e. grain 93). Ellipses 1 and 2 correspond to analysis sites 9983-93.1 and 9983-93.2 in Table 1.

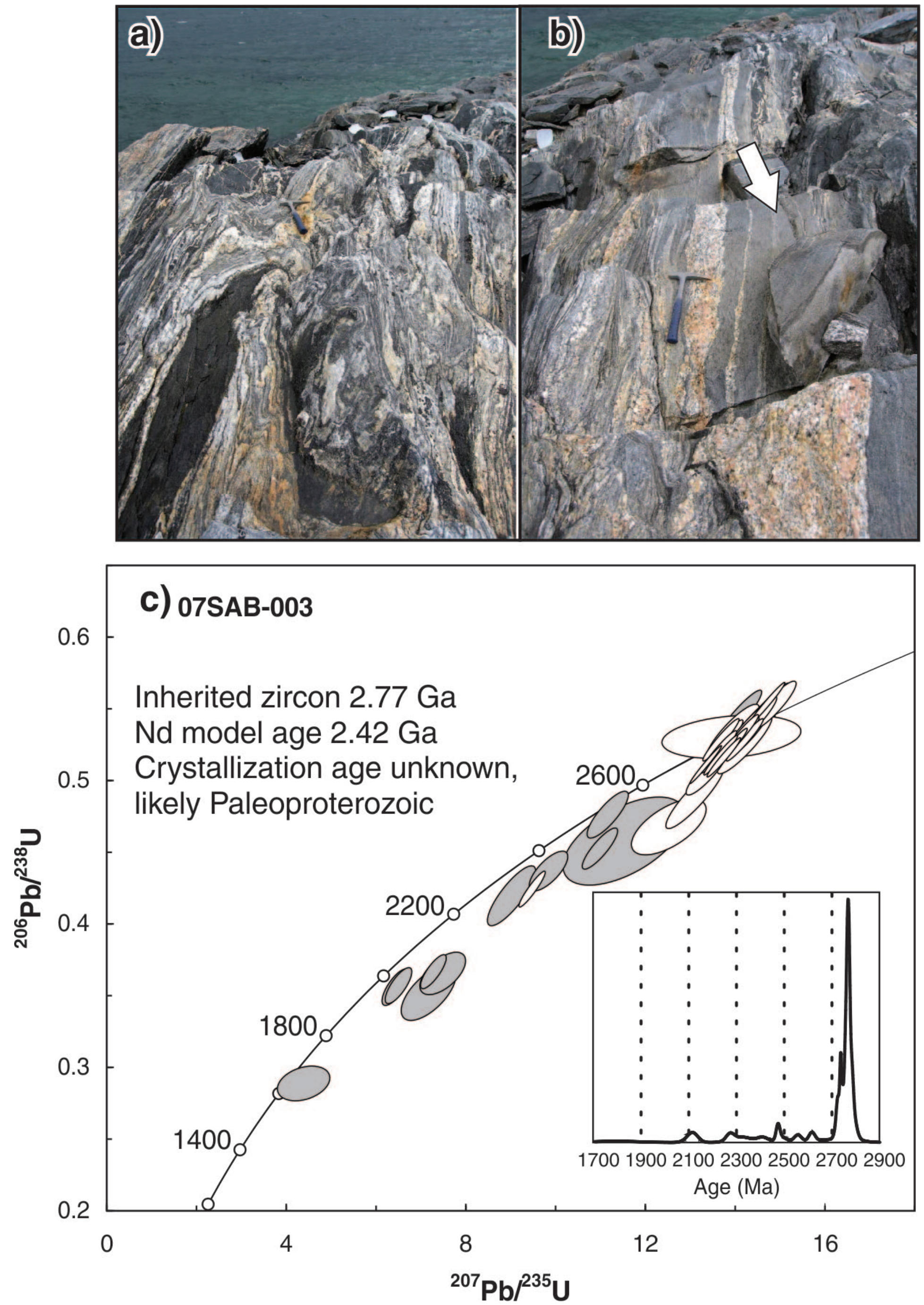

Figure 12. a) Heterogeneous nature of the gneiss complex at Cape Mercy. Hammer is approximately 30 cm. 2012-052. **b)** Homogeneous monzogranite layer (arrow) and block collected for geochronology. Hammer is approximately 30 cm. 2012-046. **c)** Concordia diagram of SHRIMP U-Pb results along with inset showing distribution of $^{207}Pb/^{206}Pb$ ages. Analyses of unzoned rims shown in grey, other analyses from inner parts of grains or zoned outer 'rims'.

The northwestern margin of the study area exposes a belt of plutonic rocks that extends over 200 km and forms the spectacular peaks of Auyuittuq National Park. Two samples from this belt yielded similar crystallization ages: biotite-hornblende-magnetite monzogranite near Pangnirtung (07SAB-002) was dated at 1894 ± 5 Ma, and biotite-hornblende-garnet granodiorite exposed 50 km northeast of Pangnirtung (09SRB-M109A) was dated at 1889 ± 3 Ma. These two ca. 1.89 Ga samples are distinctly older than the 1.865–1.845 Ga Cumberland Batholith predicted to occur in this region. Accordingly, this plutonic belt is informally designated the Qikiqtarjuaq plutonic suite. Further study will investigate whether the eastern margin of the Cumberland Batholith comprises an older ca. 1.89 Ga marginal phase represented by the Qikiqtarjuaq suite or whether any genetic association between the two exists.

Lastly, a suite of syntectonic intrusive sheets are associated with a strongly deformed corridor separating the plutonic rock–dominated domain south of the peninsula from the supracrustal rock–dominated domain north. Dated candidates of this suite include tonalite (09SRB-D10C) from within a heterogeneous gneiss unit with a maximum age of 1882 ± 13 Ma, and mylonitic K-rich aplite (09SRB-M145A) dated at 1873 ± 16 Ma. These sheets display significantly higher strain than surrounding rocks, suggesting that ca. 1.88–1.87 Ga magmatic phases were emplaced syntectonically and preferentially accommodated strain.

Neo- and Mesoarchean basement ages from Cumberland Peninsula are comparable to ages from Rae crust on northern Baffin Island and western Greenland; as is the age of the Qikiqtarjuaq suite with the 1.92–1.87 Ga Sisimiut and Arfersiorfik suites in West Greenland (Jackson et al., 1990; Wodicka et al., 2002; Bethune and Scammell, 2003; Connelly et al., 2006; St-Onge et al., 2009 and references therein). Mesoarchean basement rocks assigned to the North Atlantic craton and 1.91–1.87 Ga plutonic suites have also been identified on Hall Peninsula (Scott, 1999) and from the Torngat Orogen (Burwell Domain) in northern Labrador (Schiøtte et al., 1989; Scott, 1995). Study of the Pb-isotopic signature of these Archean rocks, as well as detailed comparison of the Hoare Bay Group with other supracrustal sequences, will hopefully clarify the affinity of the initial building blocks of the Cumberland Peninsula.

In summary, recent geological mapping supported by new isotopic and SHRIMP U-Pb geochronological data for plutonic rocks on southern Cumberland Peninsula has highlighted the presence of Archean basement to the Paleoproterozoic Hoare Bay Group, established a 200 km long belt of ca. 1.89 Ga plutonic rocks, and identified syntectonic plutonic sheets that appear to have lubricated the basement-cover contact zone during regional deformation. Collectively, these results shed light on the assembly and evolution of the eastern segment of the Trans-Hudson Orogen.

ACKNOWLEDGMENTS

Enthusiatic and able field assistance during the 2009 field season was provided by B. Hamilton, R. Keim, C. Nagy, and J. Day. Logistical support in the field was provided by Polar Continental Shelf Program (PCSP002-09) and expert air support was ensured by pilot D. Towersey with Universal Helicopters Newfoundland Ltd. M. St-Onge, R. Berman, and N. Wodicka contributed to the authors' understanding of the area through fruitful discussions both in the field and in the office. The authors thank P. Hunt, T. Pestaj, and the staff of the Geochronology Laboratory for their expert laboratory assistance. The manuscript was improved by a careful review by N. Wodicka.

REFERENCES

Bethune, K.M. and Scammell, R.J., 2003. Geology, U–Pb geochronology, and geochemistry of Archean rocks in the Eqe Bay area, north-central Baffin Island: constraints on the depositional and tectonic history of the Mary River Group of northeastern Rae Province; Canadian Journal of Earth Sciences, v. 40, p. 1137–1167. doi:10.1139/e03-028

Connelly, J.N., Thrane, K., Krawiec, A.W., and Garde, A.A., 2006. Linking the Palaeoproterozoic Nagssugtoqidian and Rinkian orogens through the Disko Bugt region of West Greenland; Journal of the Geological Society, v. 163, p. 319–335. doi:10.1144/0016-764904-115

Jackson, G.D., 1971. Operation Penny Highlands, South-Central Baffin Island; Report of Activities Part A; Geological Survey of Canada, Paper 71-1A, p. 138–140.

Jackson, G.D., Hunt, P.A., Loveridge, W.D., and Parrish, R.R., 1990. Reconnaissance geochronology of Baffin Island, N.W.T.; *in* Radiogenic age and isotopic studies: Report 3; Geological Survey of Canada, Paper 89-2, p. 123–148.

Ludwig, K.R., 2003. User's manual for Isoplot/Ex rev. 3.00: a Geochronological Toolkit for Microsoft Excel; Special Publication, 4, Berkeley Geochronology Center, Berkeley, California, 70 p.

Sanborn-Barrie, M., Young, M., and Whalen, J., 2011a. Geology, Kingnait Fiord, Nunavut; Geological Survey of Canada, Canadian Geoscience Map 2 (2nd edition, preliminary), scale 1:100 000. doi:10.4095/289238

Sanborn-Barrie, M., Young, M., Whalen, J., and James, D., 2011b. Geology, Ujuktuk Fiord, Nunavut; Geological Survey of Canada, Canadian Geoscience Map 1 (2nd edition, preliminary), scale 1:100 000. doi:10.4095/289237

Sanborn-Barrie, M., Young, M., Whalen, J., James, D., and St-Onge, M.R., 2011c. Geology, Touak Fiord, Nunavut; Geological Survey of Canada, Canadian Geoscience Map 3 (2nd edition, preliminary), scale 1:100 000. doi:10.4095/289239

Schiøtte, L., Compston, W., and Bridgwater, D., 1989. Ion probe U-Th-Pb zircon dating of polymetamorphic orthogneisses from northern Labrador, Canada; Canadian Journal of Earth Sciences, v. 26, p. 1533–1556. doi:10.1139/e89-131

Scott, D.J., 1995. U-Pb geochronology of the Nain craton on the eastern margin of the Torngat Orogen, Labrador; Canadian Journal of Earth Sciences, v. 32, p. 1859–1869.

Scott, D.J., 1999. U-Pb geochronology of the eastern Hall Peninsula, southern Baffin Island, Canada: a northern link between the Archean of West Greenland and the Paleoproterozoic Torngat Orogen of northern Labrador; Precambrian Research, v. 93, p. 5–26. doi:10.1016/S0301-9268(98)00095-3

St-Onge, M.R., Jackson, G.D., and Henderson, I., 2006. Geology, Baffin Island (south of 70°N and east of 80°W), Nunavut; Geological Survey of Canada, Open File 4931, scale 1:500 000.

St-Onge, M.R., Van Gool, J.A.M., Garde, A.A., and Scott, D.J., 2009. Correlation of Archaean and Palaeoproterozoic units between northeastern Canada and eastern Greenland: constraining the pre-collisional upper plate accretionary history of the Trans-Hudson orogen; Geological Society, London, Special Publication 2009, v. 318, p. 193–235. doi:10.1144/SP318.7

Stern, R.A., 1997. The GSC Sensitive High Resolution Ion Microprobe (SHRIMP): analytical techniques of zircon U-Th-Pb age determinations and performance evaluation; *in* Radiogenic Age and Isotopic Studies: Report 10; Geological Survey of Canada, Current Research 1997-F, p. 1–31.

Stern, R.A. and Amelin, Y., 2003. Assessment of errors in SIMS zircon U-Pb geochronology using a natural zircon standard and NIST SRM 610 glass; Chemical Geology, v. 197, p. 111–142. doi:10.1016/S0009-2541(02)00320-0

Whalen, J.B., Wodicka, N., Taylor, B.E., and Jackson, G.D., 2010. Cumberland batholith, Trans-Hudson Orogen, Canada: Petrogenesis and implications for Paleoproterozoic crustal and orogenic processes; Lithos, v. 117; Issues (National Council of State Boards of Nursing (U.S.)), v. 1–4, no. June, p. 99–118.

Wodicka, N., St-Onge, M.R., Scott, D.J., and Corrigan, D., 2002. Preliminary report on the U-Pb geochronology of the northern margin of the Trans-Hudson Orogen, central Baffin Island, Nunavut; *in* Radiogenic Age and Isotopic Studies: Report 15; Geological Survey of Canada, Current Research 2002-F7, 12 p. doi:10.4095/213623

Geological Survey of Canada Project MGM 007